Applied Superconductivity Center
University of Wisconsin -Madison
Madison , WI 53706

December 1990

"ASTROMAG"
COIL COOLING STUDY

by

Ben-Zion Maytal *

Steven W. Van Sciver

Supported by

NASA GODDARD SPACE CENTER
Greenbelt , MD
Contract (Research Grant) No: NAG5-1417

* On sabbatical leave from RAFAEL and TECHNION-
Israeli Institute of Technology , Haifa , Israel

Table of Contents

6. PRELIMINARY DESIGN ATTEMPT

7. HE II INTERNAL CONVECTION COOLING SYSTEM

8. HOFMANN LOOP SYSTEM

Nomenclature

A	area [m^2]
A_s	cross-section area of a conducting thermal strap [m^2]
A_v	convective heat transfer area of vapor cooling [m^2]
D	pipe diameter [m]
d	diameter of capillary pores [m]
c_m	specific heat of magnet [J kg^{-1} K^{-1}]
c_p	specific heat at constant pressure of helium [J kg^{-1} K^{-1}]
$f(T)$	temperature dependent helium II conductivity function [cm^5 K W^{-3}]
f	hydrodynamic friction factor, non-dimensional
$g(T)$	$\dfrac{c_m}{\dfrac{k\,c_p}{\lambda}(T - T_b)^2 + \dfrac{k}{1 + \dfrac{k}{hL}}(T - T_b)}$ [s m kg^{-1} K^{-1}]
h	convection heat transfer coefficient [W m^{-2} K^{-1}]
h_b	boiling heat transfer coefficient [W m^{-2} K^{-1}]
h_c	constant heat transfer coefficient [W m^{-2} K^{-1}]
h_k	Kapitza's heat conduction coefficient [W m^{-2} K^{-1}]
I_1	$\int_2^{T_{quench}} y(T)\,dT$
I_2	$\int_2^{T_{amb}} y(T)\,dT$

k	thermal conductivity [W m^{-1} K^{-1}]
K	non-dimension parameter, $\rho\ c_p\ v\ (f\ L)^{-1}\ \Delta T^{2/3}$, expressing the ratio of external and internal convective heat transport in He II
L	length [m]
m	mass [Kg]
$\dot{m}$	vapor mass flowrate [kg s^{-1}]
Nu	Nusselt Number, hL/k
P	pressure [Pa]
$\dot{q}$	heat flux [W m^{-2}]
$\dot{Q}$	heat power [W]
$\dot{Q}_{HX}$	rate of heat transfer in vapor heat exchanger [W]
$\dot{Q}_{peak}$	peak heat flux through thermal straps at T_{amb} while cooling down
$\dot{Q}_{strap}$	heat transporting rate through strap to bath [W]
R	thermal resistance, $\Delta T/\dot{Q}$ [K W^{-1}]
s	entropy [J $mole^{-1}$ K^{-1}]
t	time [s]
t_{CD}	cooling down time [s]
Δt_1	cooling down period from quench [s]
Δt_2	cooling down period from ambient [s]
T	absolute temperature [K]
T_o	thermal strap low end temperature [K]
T_b	helium bath temperature [K]

T_{amb} ambient temperature [K]

T_{in} vapor heat exchanger inlet temperature [K]

T_{out} vapor heat exchanger outlet temperature [K]

T_m magnet temperature [K]

T_{quench} magnet temperature at quench [K]

ΔT temperature difference [K]

ΔT_{boil} temperature drop at the cold end of thermal strap, across the boiling film [K]

ΔT_K temperature drop on Kapitza's conductivity [K]

v velocity [m s^{-1}]

v_g specific volume of vapor [m^3 $mole^{-1}$]

v_n normal fluid velocity [m s^{-1}]

V volume [m^3]

x linear coordinate (along thermal strap [m]

$y(T)$ $\dfrac{c_m(T)}{k(T)\,(T - T_b)}\left(1 + \dfrac{1}{Nu}\right)$ [s m g^{-1} K^{-1}]

Z $A_s/(A_s + Nu^* A_v)$

Greek letters

α thermal diffusivity, $k/(\rho c)$ [m^2 s^{-1}]

β geometric factor

δ	thickness of a cylindric shell [m]
η	viscosity [N s m^{-2}]
λ	latent heat of evaporation [J kg^{-1}]
ρ	density [kg m^{-3}]
μ	chemical potential [J $mole^{-1}$]

Subscripts

amb	ambient
av	average
fe	fountain effect pump
m	magnet
n	normal fluid
min	minimum
s	super fluid
st	thermal strap
svp	saturation conditions
v	vapor

LIST OF FIGURES

Fig. 13: Thermal strap cold end temperature while magnet cooling down, as function of magnet's temperature.

Fig. 14: Layout and notation of magnet cooling down by thermal strap and vapor heat exchanger.

Fig. 15: Aluminum, $g = \dfrac{c_m}{\frac{kc_p}{\lambda}(T - T_b)^2 + \frac{khL}{K + hL}(T - T_b)}$ as function of T.

Fig. 16: Restrictive sizing characteristics of aluminum thermal strap at various modes of operation.

Fig. 17: Restrictive sizing characteristics of copper thermal strap at various modes of operation.

Fig. 18: Preliminary design attempt of a thermal strap.

Fig. 19: Schematic representation of He II Heat Pipe system for ASTROMAG.

Fig. 20: Porous plug operation described in terms of liquid helium phase diagram.

Fig. 21: Block diagram linearized representation of Hofmann's Cooling Loop for system stability analysis.

INTRODUCTION

1.1 ASTROMAG - General Review

ASTROMAG is a planned Particle Astrophysics Magnet Facility. Basically it is a large magnetic spectrometer outside the Earth's atmosphere for an extended period of time in orbit on a space station. A Definition Team[1] summarized its scientific objectives assumably related to fundamental questions of astrophysics, cosmology and elementary particle physics.

Since magnetic induction of about 7 Tesla is desired, it is planned to be a superconducting magnet cooled to liquid He II temperatures.

The general structure of ASTROMAG is based on:

a. Two superconducting magnet coils.

b. Dewar of liquid He II to provide cooling capability for the magnets.

c. Instrumentation: magnet spectrometer

   1. Matter-Anti Matter Spectrometer (MAS)

   2. Cosmic Ray Isotope Spectrometer (CRIS)

d. Interfaces to the shuttle and space station.

Many configurations[5-7] of the superconducting magnets and the dewar have been proposed and evaluated, since those are the heart of the ASTROMAG. Baseline of

the magnet configuration and cryostat as presented in phase A study[2] and the one kept in mind will doing the present study is shown in Figs. 1 and 2.

Resupply is assumed to take place every 12 to 24 months assuming a cryostat design to hold sufficient helium for 2 ÷ 4 years operation.

ASTROMAG's development schedule reflects the plan of launching to space station in 1995.

1.2 Cooling System Specification

Based on sources (2) and (3) the magnet coil cooling system must operate under five distinct conditions. These are in order of importance.

1.2.1 Magnet charging

1.2.1.1 While the magnets are being charged, their temperature should be 1.4 - 1.8 K.

1.2.1.2 Power dissipation in each of the coils will be approximately 250 mW.

1.2.1.3 Dissipation in the persistent switch will be approximately 2.0 W.

1.2.2 Charged operation

1.2.2.1 The magnet coils should be at 1.4 ÷ 1.8 K.

1.2.2.2 Parasitic heat input to each coil plus field decay totals approximately 10 mW.

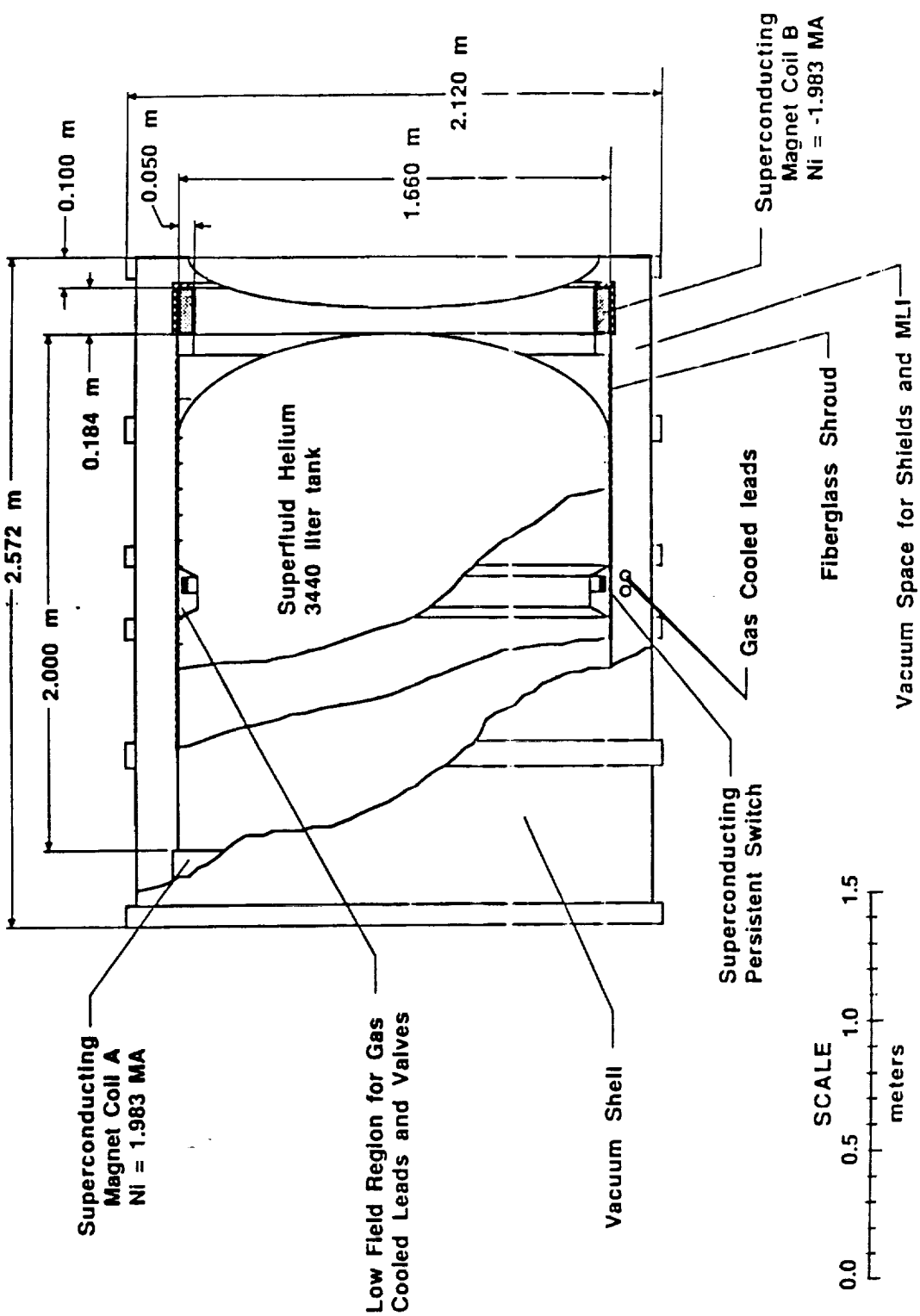

Fig. 1: Baseline ASTROMAG magnet cryostat.[2]

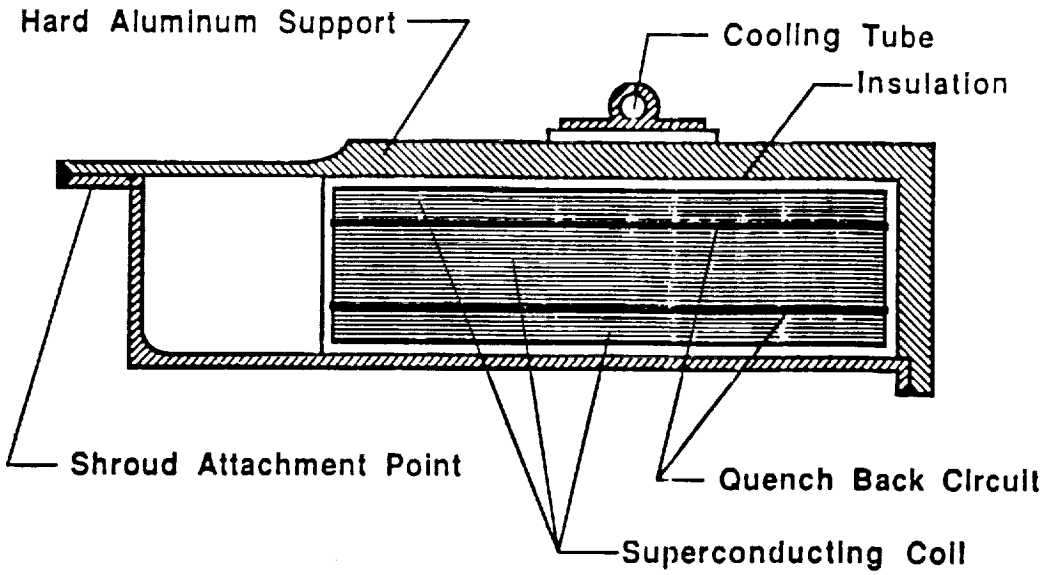

COPPER BASELINE MAGNET PARAMETERS

Number of Magnet Coils	2
Number of S/C Layers per Coil	34
Number of QB Layers per Coil	4
Number of Turns per Layer	72
Number of S/C turns per Coil	2448
Number of QB turns per coil	288
Coil Outside Diameter (m)	1.66
Coil Inside Diameter (m)	1.56
Space Between the Coils (m)	2.00
Coil Width (mm)	184.00
Magnet Self Inductance (H)	33.52
11 MJ Design Current (A)	810.09
Coil Peak Induction (T)*	6.74
Intercoil Tensile Force (kN)*	251#
S/C Matrix Current Density (A/ sq mm)*	405
Quench Energy at 1.8 K (micro-joules)	9.6

* At the 11 MJ Design Coil Current
\# 25.6 metric tons

Fig. 2: Copper baseline superconducting coil.[2]

1.2.2.3 Total stored energy is 11 MJ.

1.2.2.4 Parasitics on the cryogen tank from other sources total approximately 60 mW.

1.2.3 Magnet quench

1.2.3.1 The magnetic field drops to zero in 2-5 seconds.

1.2.3.2 The coil temperature rises to 100-120 K.

1.2.3.3 Following a quench, enough He II should remain in the tank to allow a magnet cooldown and resumption of normal operation.

1.2.3.4 The temperature in the cryogenic tank must not exceed the lambda point at any time while there is helium left in the tank.

1.2.3.5 The goal is a maximum temperature in the tank of 1.95 K.

1.2.4 Cooldown from room temperature

The coil cooling system should bring the temperature of the coils to below 2.0 K within 72 hours.

1.2.5 Post quench cooldown

The coil cooling system should return the temperature of the coils to below 2 K within 48 hours after the quench.

1.2.6 As a design goal the dewar and the cooling system should be capable for 4 years operation.

1.3 Scope of Study

1.3.1 Thermal straps

Detailed study of materials and sizes for steady state and transient analysis.

1.3.2 Thermal straps and vapor cooling

1.3.3 Hofmann's Loop System

That concept[14-17] is one of the ASTROMAG's leading designs. Based on published analysis and experiments in addition to theoretical considerations, its main parameters to meet the requirements are derived.

1.3.4 Suggestion: He II internal convection cooling

A basic comparison is drawn between internal and external convection to evaluate the necessity of the last one. Demonstrating feasibility of the internal convection, a general description of the proposed system is derived.

2. STEADY STATE ANALYSIS

2.1 Assumptions

2.1.1 General layout and notation, on Fig. 3.

2.1.2 There are two separate magnetic coils, each thermally coupled to cryogenic bath.

2.1.3 The upper limit of bath temperature has to meet the required lowest temperature which is 1.4 K - 1.8 K at charging.

2.1.4 Sharing temperatures drop, on Fig. 4.

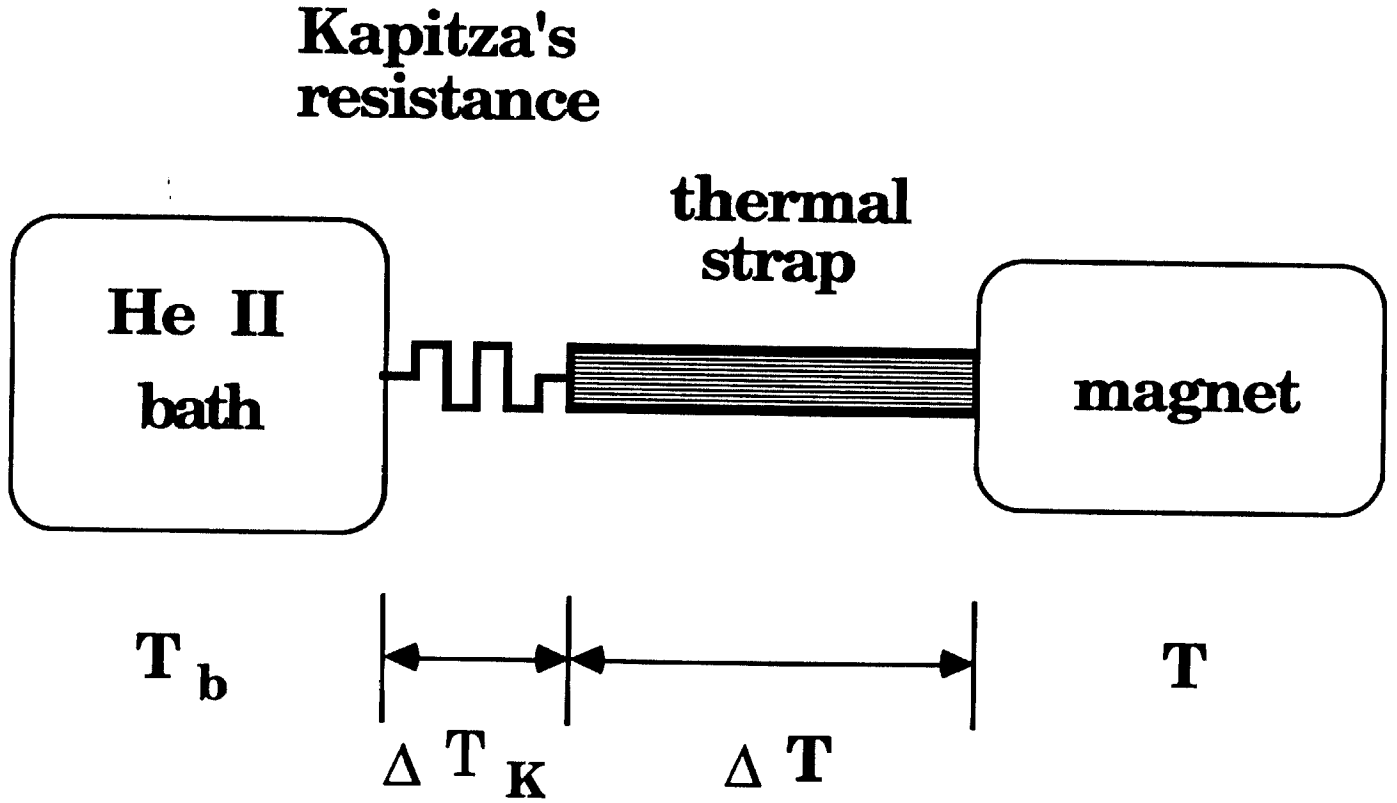

Fig. 3: Steady state thermal model and notation.

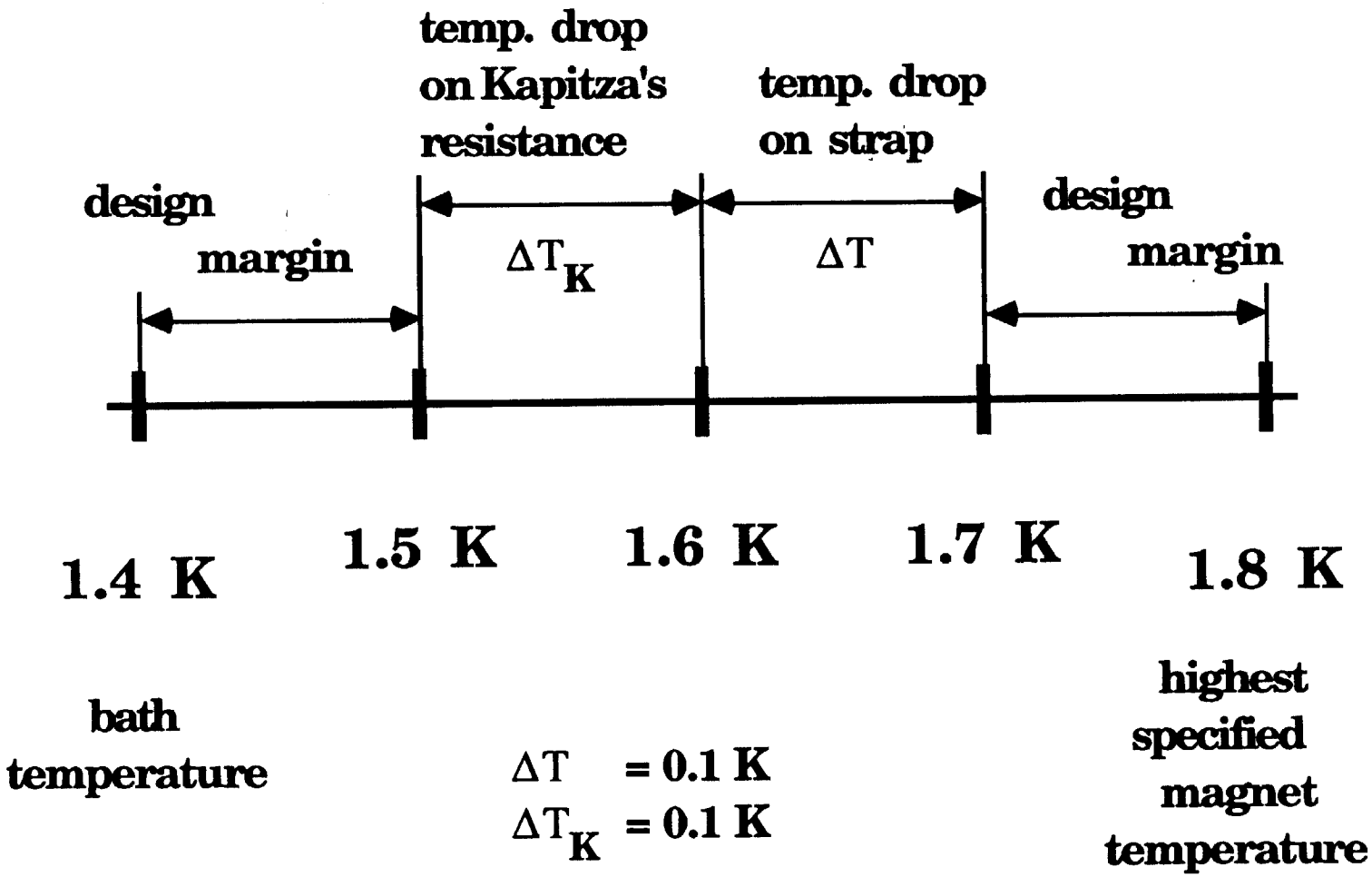

Fig. 4: Sharing temperature drop on steady state.

2.2 Mathematical Model

2.2.1 Fourier's equation

$$q = k \frac{dT}{dx}$$

or

$$\frac{\dot{Q}}{A} = k \frac{dT}{dx}$$

At steady state there is an almost linear profile because in the small range of ΔT = 0.1 K the k is quite constant as shown in Fig. 5.

$$\frac{dT}{dx} = \frac{\Delta T}{L}$$

$$\frac{A}{L} = \frac{\dot{Q}}{k * \Delta T}$$

2.2.2 The highest heat load occurs during the charging mode. The dissipation in each coil is: 0.25 W.

2.2.3 A higher value of A/L means that for a given cross section area, A, a shorter strap is required for the job, and v.v.

2.2.4 The above A/L value is the minimal one (representing the longest strap). Higher values might be used.

2.3 Copper (RRR = 100)

$$k(1.5\ K) = 2.5\ W\ cm^{-1}\ K^{-1}$$

$$\frac{A}{L} = \frac{0.25\ W}{2.5\ \frac{W}{cm\ K} * 0.1\ K} = 1.0\ cm$$

2.3.1 Example

For a cylindric shell of D = 200 cm and thickness of δ = 0.5 cm its length should not exceed:

$$L = \frac{200 * 3.14\ cm * 0.5\ cm}{1.0\ cm} = 314\ cm$$

For δ = 2 cm, L = 78.5 cm.

2.3.2 Example

For one large coil instead of two with a double dissipation we get a maximum half length: 157 cm.

2.3.3 Summary

Under the steady state requirement it seems that there is no practical limitation on the minimal length of the thermal strap.

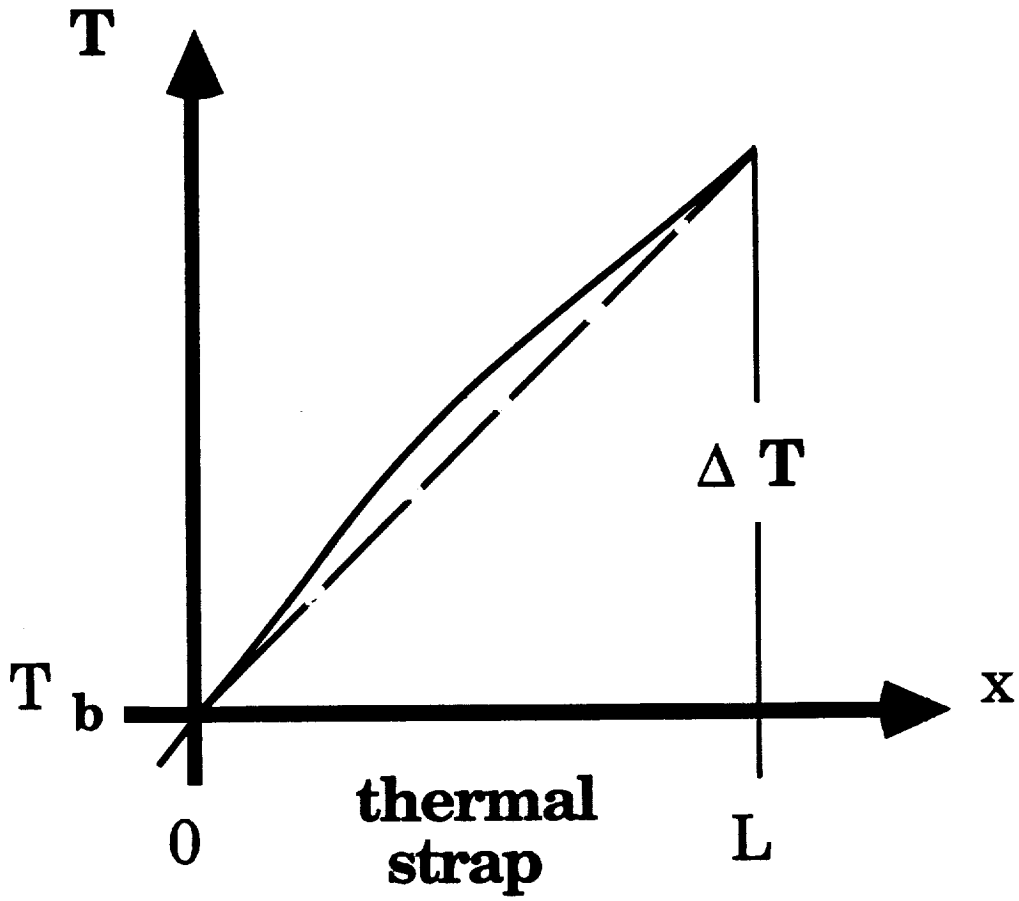

Fig. 5: Steady state (qualitative) temperature profile along the thermal strap.

2.4 Aluminum (1100 F)

$$k\,(1.5\ K) = 0.15\ \frac{W}{cm\ K}$$

2.4.1

$$\frac{A}{L} = \frac{0.25\ W}{0.15\ \frac{W}{cm\ K} * 0.1\ K} = 16.7\ cm$$

Example

Cylindrical shell D = 200 cm, δ = 0.5 cm, the maximum length:

$$L = 18.8\ cm$$

(It's mass is 15.93 kg.)

2.4.2 Stainless steel type 304

$$k\,(1.5\ K) = 0.0008\ \frac{W}{cm\ K}$$

$$\frac{A}{L} = \frac{0.25}{0.0008 * 0.1} = 3125\ cm$$

For a concept of supporting structural load by the cooling strap so that: $\delta = 5$ cm for a cylindrical shell of D = 200 cm.

$$L = \frac{200 * 3.14 * 5}{3125} = 1.0 \text{ cm}$$

(It's mass is 25 kg.)

2.4.3 Aluminum 5083

$$k\,(1.5\ K) = 0.015\ \frac{W}{cm\ K}$$

$$\frac{A}{L} = \frac{0.25}{0.015 * 0.1} = 1.67 \text{ cm}$$

2.4.4 High purity aluminum RRR = 1500

$$k\,(1.5\ K) \sim 15\ \frac{W}{cm\ K}$$

$$\frac{A}{L} = 0.17 \text{ cm}$$

2.5 Kapitza's Thermal Resistance

$$h_k = 0.04\ T^3\ \frac{W}{cm^2\ K}$$

$$h_k = \frac{q}{\Delta T} = \frac{\dot{Q}}{A * \Delta T} \qquad A = \frac{\dot{Q}}{h_k * \Delta T}$$

$$@\ 1.5\ K \qquad h_k = 0.135\ \frac{W}{cm^2\ K}$$

For

$$\dot{Q} = 0.25\ W \quad \text{and} \quad \Delta T_k = 0.1\ K$$

$$A = \frac{0.25\ W}{0.135 \frac{W}{cm^2\ K} * 0.1\ K} = 18.5\ cm^2$$

A cylindric shell of D = 200 cm has that cross section area for δ = 0.03 cm. It means that a very small area is enough for providing a low Kapitza's resistance.

2.6 Vapor Contact

Under conditions of low gravity the He II might be distributed inside the dewar so that the cold end of the strap contacts vapor. In this case the heat transfer coefficient is of boiling. A low value of film boiling heat transfer coefficient[4] is:

$$h = 0.02 \frac{W}{cm^2 K}$$

The worst case is when exactly the whole cross section area of the strap is exposed to vapor. If less is exposed then the h of boiling is replaced by that of Kapitza's conductance which has a higher value. If a larger area is exposed to vapor then the equivalent heat transfer coefficient h A is bigger again.

$$A_{min} = \frac{\dot{Q}}{\Delta T * h} = \frac{0.25\ W}{0.1\ K * 0.02 \frac{W}{cm^2 K}} = 125\ cm^2$$

2.7 Thermal Conductivity in Magnetic Field

Thermal conductivity, more apparent for high purity metals, tends to decrease sharply under magnetic field. So far the available data are for Al RRR = 1500 up to 4.0 Tesla and down to 7.0 K.[9] The present need for data goes down to 1.5 K. It is hard to extrapolate, however it is possible to draw the following trends.

1. At low temp. (under 50 K) the k decreases with temp.
2. For Al RRR = 1500, at 7.0 K, at 4 Tesla, the k is reduced by a factor of 8.7/2.9 = 3.0, compared to 0 Tesla field. The change from 3 Tesla to 4 Tesla at 7.0 K is only 3.02/2.93 = 1.03 (source No. 9 p. 152).
3. The field dependence of k exhibits a saturational behavior which practically means that no more decrease occurs under higher field.
4. Toward 0 K the k approaches exponentially close to zero values. Therefore, under topological reasoning of the B dependence of k we may conclude:

$$\text{for Al RRR = 1500 at 1.5 K:} \qquad \frac{k\ (4\ \text{Tesla})}{k\ (0\ \text{Tesla})} = \frac{1}{3}$$

At 1.5 K for H.P. Al extrapolated from source No. 8 about Aluminum 1 is:

$$k\ (0\ \text{Tesla},\ 1.5\ \text{K}) = 15\ \frac{\text{W}}{\text{cm K}}$$

So assumably under previous conclusions:

$$k\ (7\ \text{Tesla},\ 1.5\ K) = 5\ \frac{W}{cm\ K}$$

$$\left(\frac{A}{L}\right)_{H.P.\ Al} = \frac{0.25}{5 * 0.1} = 0.5\ cm$$

For H.P. annealed copper through extrapolation from 4 K to 1.5 K (source No. 8)

$$k\ (0\ \text{Tesla},\ 1.5\ K) = 30\ \frac{W}{cm\ K}$$

Assumably, again under the same degradation through magnetic field:

$$k\ (7\ \text{Tesla},\ 1.5\ K) = 10\ \frac{W}{cm\ K}$$

$$\left(\frac{A}{L}\right)_{H.P.\ Annealed\ Cu} = 0.25\ cm$$

Through sources (5) and (7) the ASTROMAG magnetic field is assumably about 7 Tesla.

2.8 Mixed Case (Example)

Assuming that the ends of the strap are to be of the structural alloy Al 5083 and its heart of H.P. Al as shown on Fig. 6.

By source ( ) for Al-Al electropolished contacts at 4.2 K > T > 1.8 K

$$h_2 = 3.6 * 10^{-3} T^{2/3} \frac{W}{cm^2 K}$$

Applying the above relation for 1.5 K

$$h_2 = 0.005 \frac{W}{cm^2 K}$$

$$h_1 = 0.02 \frac{W}{cm^2 K}$$

The altogether thermal resistance R

$$R = \frac{L_1}{K_1 * A} + \frac{L_2}{K_2 * A} + \frac{L_3}{K_1 * A} + \frac{1}{h_1 * A} + \frac{2}{h_2 * A}$$

when

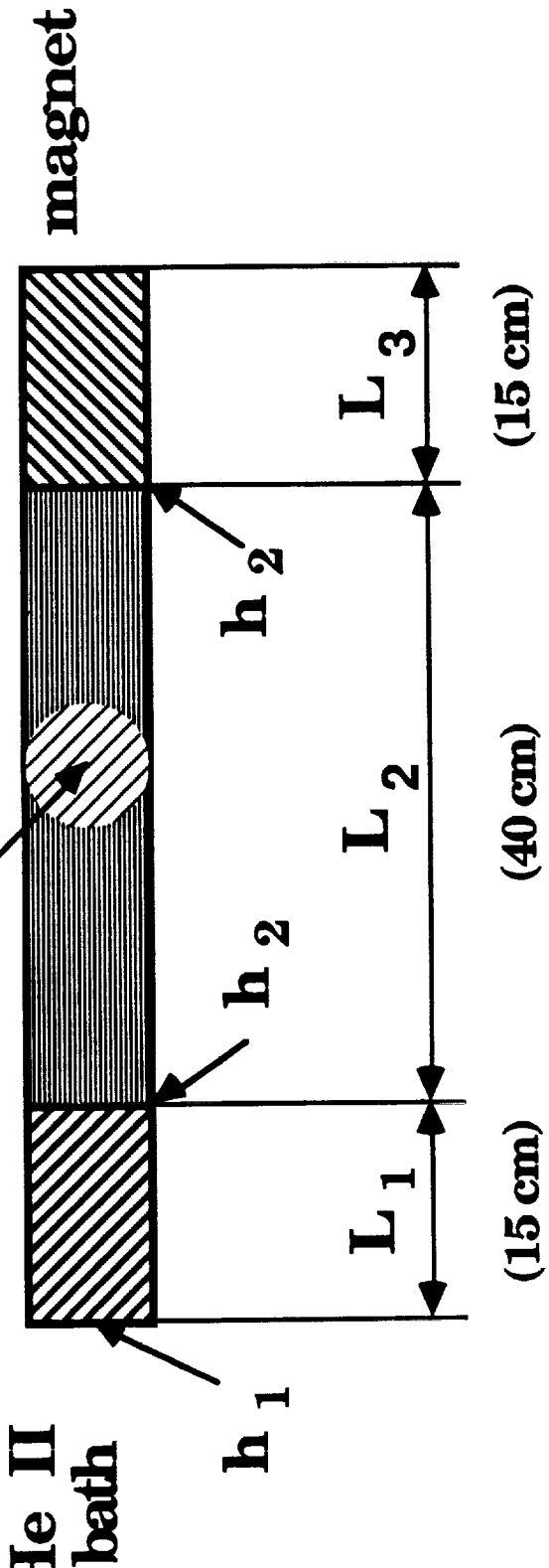

Fig. 6: Example of a two material composed thermal strap.

$$R * \dot{Q} = \Delta T$$

For our case: (Phase A design)

$$R = \frac{15}{0.015\ A} + \frac{40}{5\ A} + \frac{15}{0.015\ A} + \frac{1}{0.02\ A} + \frac{2}{0.005\ A} =$$

$$\frac{1}{A}\left[1000 + 8 + 1000 + 50 + 400\right] = \frac{2458}{A}\ \frac{K}{W}$$

$$R = \frac{\Delta T}{\dot{Q}} \qquad A = \frac{2458\ \dot{Q}}{\Delta T} = \frac{2458 * 0.25}{0.1} = 6145\ cm^2$$

For D = 200 cm δ = 9.7 cm.

The main contribution comes from the high thermal resistance of the Al 5083 and the contact resistance.

Conclusions

1. The ends of the strap have to be as short as possible, like 3 cm each one.
2. The contact thermal resistance has to be specially designed by enlarging the contact area.

Improved design: (Phase B)

$L_1 = L_3 = 3$ cm $\qquad A_{contact} = 2\ A$

$$R = \frac{1}{A}\left[200 + 8 + 200 + 50 + 200\right] = \frac{658}{A}$$

$$A = \frac{658 * 0.25}{0.1} = 1645\ cm^2$$

@ D = 200 cm, $\qquad \delta = 2.6$ cm

Phase C

$L_1 = L_2 = 1$ cm $\qquad A_1 = A_2 = 2\ A \qquad A_{contact} = 2\ A$

$$R = \frac{1}{A}\left[50 + 8 + 50 + 25 + 200\right] = 433/A$$

A = 1083 cm, $\qquad$ @ D = 200 cm $\qquad \delta = 1.7$ cm

3. TRANSIENT ANALYSIS: COOLING DOWN THROUGH ONLY

3.1 Assumptions

3.1.1 General layout, on Fig. 7

T(t) - temperature of the magnet as a lamped mass, and the high temperature of the strap.

T_o - the low temperature of the strap

3.1.2

$T_o = T_b + \Delta T_{boil}$

T_b, bath temp.

ΔT_{boil}, temp. drop at the boiling film.

3.1.3 Temperature profiles along the strap are qualitatively derived from the heat conduction factor (k) temperature dependence, as shown in Fig. 8.

Assuming developed profiles or the quasi static case:

$$q \neq f(x)$$

$$k \frac{dT}{dx} = q = \text{Const}$$

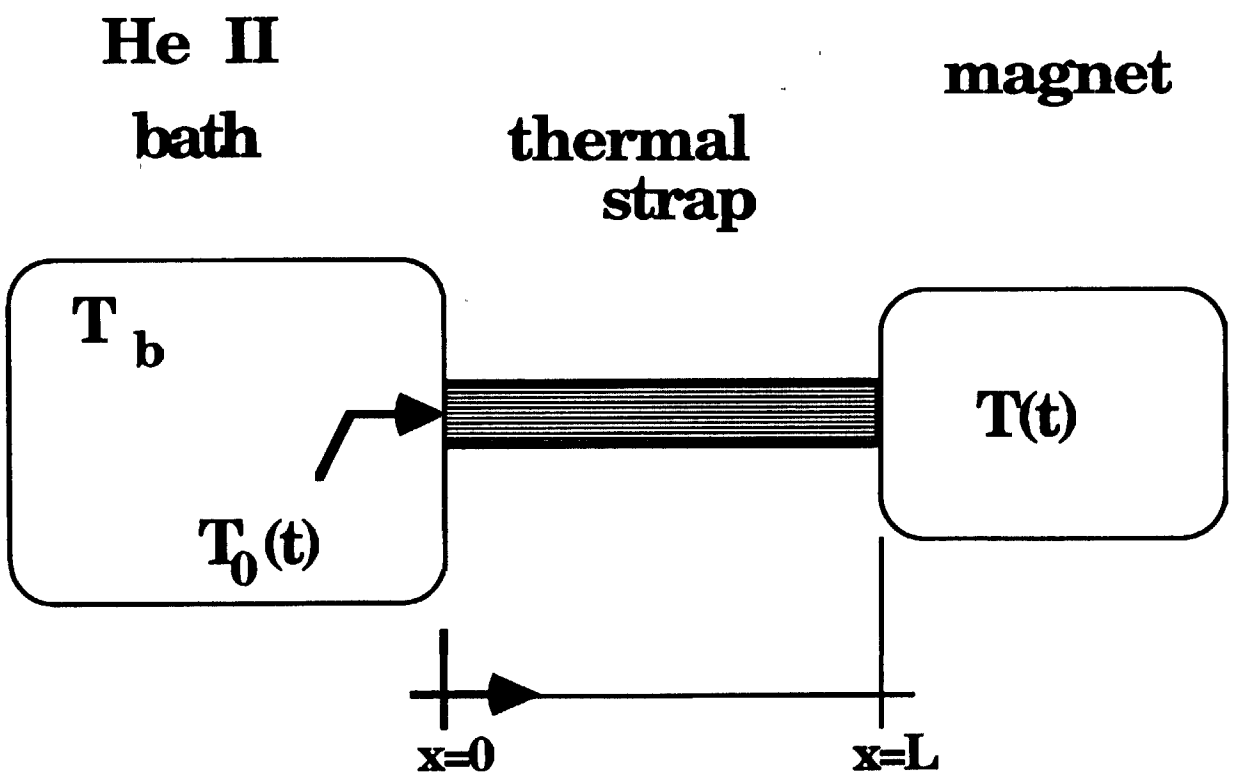

Fig. 7: General layout and notation for transient analysis of magnet cooling down through thermal strap.

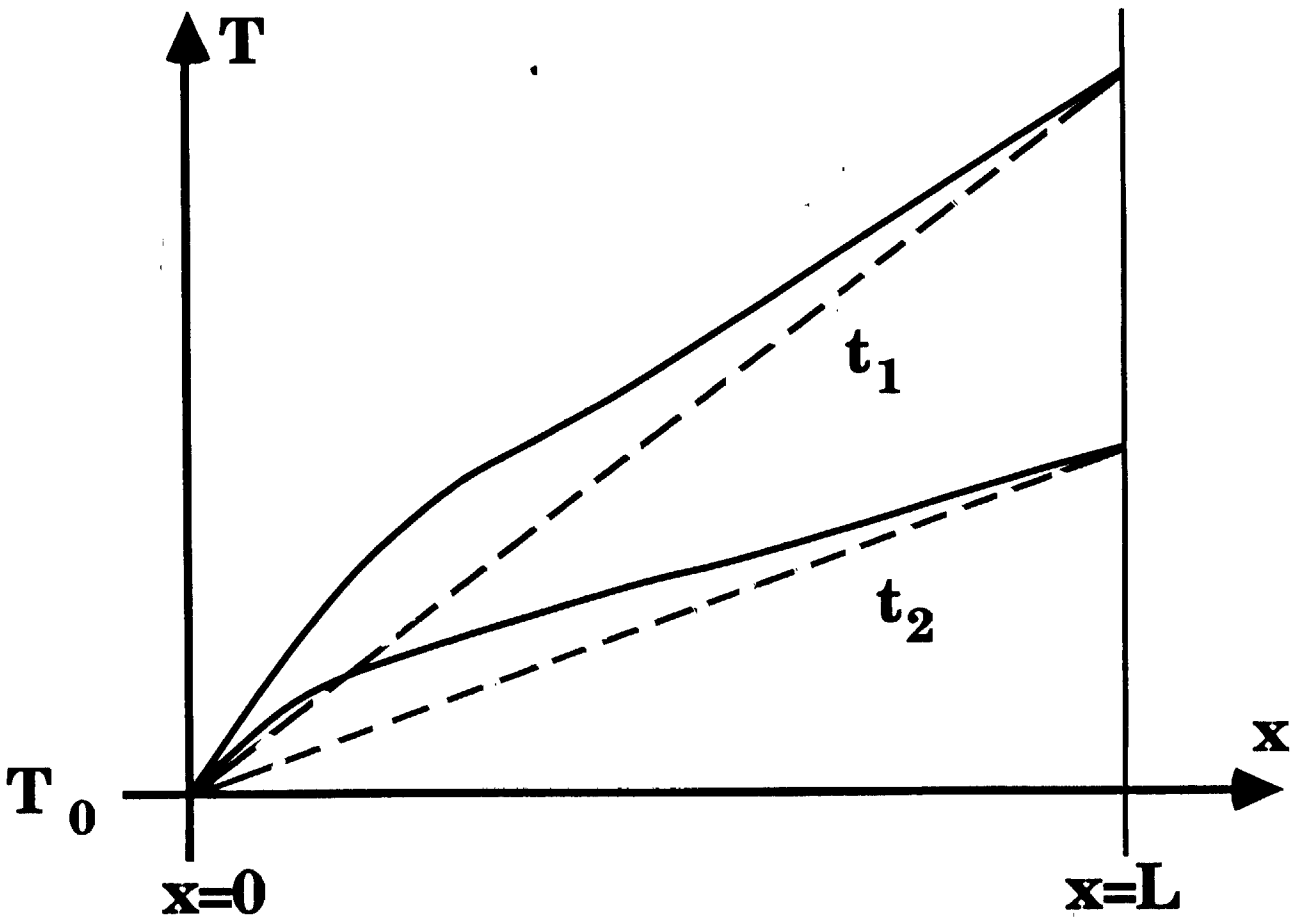

Fig. 8: Transient (qualitative) temperature profiles of magnet cooling down through thermal strap.

$$\frac{dT}{dx} = \frac{q}{k}$$

For low k, dT/dx is large and v.v.

3.1.4 Developed temperature profiles

The non-dimensional time parameter $(\alpha t/l^2) \sim 0.5$ can serve as a criteria for the quasi static (developed) case.

$$\alpha, \text{ thermal diffusivity, } \frac{k}{\rho c}$$

$$t = \frac{l^2}{\alpha} 0.5$$

Assuming L = 15 cm, for copper RRR = 100

$$\text{@ 300 K:} \qquad \alpha = \frac{k}{\rho c} = \frac{0.42 \ \frac{W}{cm\ K}}{8.96 \ \frac{g}{cm^3} * 0.38 \ \frac{J}{g\ K}} = 0.12 \ \frac{cm^2}{s}$$

$$t = \frac{0.5 * 225\ cm^2}{0.12\ cm^2/s} = 937 s = 15.6\ min$$

For Al (1100)

@ 300 K: $\alpha = \frac{2.1}{2.7 * 0.902} = 0.86\ cm^2/s$

$$t = \frac{0.5 * 225}{0.86}\ s = 130 s \sim 2\ min$$

The cooling process is much longer ($2.59 * 10^5$ sec or 4320 min) so under that resolution of time it might be justified to concern it as a quasi static case.

3.1.5 The straight line temperature profile serves in this case a guideline or a frame for the exact solution because:

1. for k independent on T the developed solution is linear (for any value of constant k)
2. over a wide range of T (100-300 K) the thermal conductivity is almost constant.

3.1.6 Boiling

While cooling down the rate of heat removal is much higher than at steady state, the average power for 72 hours of cooling down is:

$$\dot{Q}_{av} = \frac{26 * 10^6 J}{2.5 * 10^5 s} = 100.4 \text{ W}$$

A typically low value of film boiling heat transfer coefficient is:

$$h = 0.02 \frac{W}{cm^2 K}$$

defined through:

$$q = h * \Delta T$$

For the practical case of D = 200 cm and δ = 0.5 cm

$$q_{av} = \frac{100.4 \text{ W}}{314 \text{ cm}^2} = 0.318 \frac{W}{cm^2}$$

$$\Delta T_{av} = \frac{q}{h} = \frac{0.318 \frac{W}{cm^2}}{0.02 \frac{W}{cm^2 K}} = 15.9 \text{ K} \equiv \Delta T_{boil}$$

Assuming that the average heat flux is reached at 150 K, the ΔT_{av} = 15.9 K is quite non-negligible. Notation shown in Fig. 9.

Conclusion:

The cooling down strap conduction should be solved coupled with the boiling process.

3.1.7 The magnet might be concerned as made mainly of copper, though its mass of 650 kg and storing 11 MJ which raises its temp. to 120 K.

For copper:

$$m \int_2^{120} c \, dT = 650 \; 10^3 \; g \; 17 \; \frac{J}{g} = 11.05 \; MJ$$

3.1.8 Total internal energy remove is derived through temperature extension to 300 K

$$\Delta E = m \int_2^{300} c \, dT = 650 * 10^3 \; g \; 40 \; \frac{J}{g} = 26 \; MJ$$

3.1.9 The mass of the strap is negligible compared to the mass of the magnet.

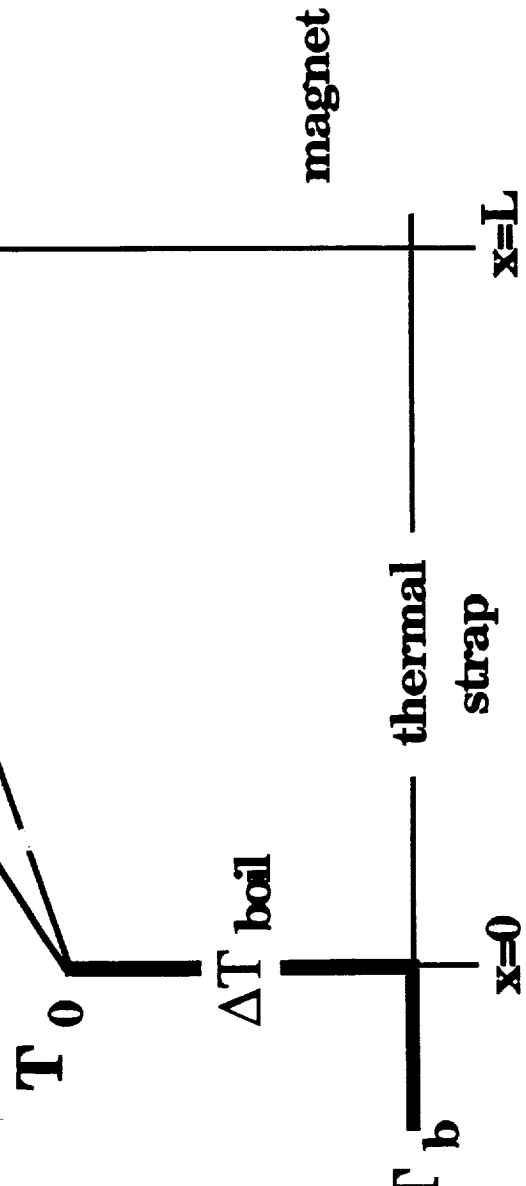

Fig. 9: Temperature drop across the boiling film and profile while magnet cooling down.

3.2 Mathematical Model

3.2.1 The heat flux at the hot end of the strap, q(L), represents the cooling rate of the magnet dT/dt.

$$V_m \rho_m c_m \frac{dT}{dt} = A\, q(L) = -k\, A \left(\frac{dT}{dx}\right)_{x=L}$$

The index m refers to magnet.

3.2.2 Basic assumption of the model (discussed later)

$$\left(\frac{dT}{dx}\right)_{x=L} \cong \frac{\Delta T}{L} = \frac{T - T_o}{L}$$

3.2.3 The ruling differential equation

$$V_m \rho_m c_m \frac{dT}{dt} + \frac{kA}{L}(T - T_o) = 0$$

That is a first order, non-linear diff. equation. Its coefficients are temperature dependent.

3.2.4 Through 3.1.2 and 3.1.6:

$$T_o = T_b + \Delta T_{boil} = T_b + \frac{q(x=0)}{h}$$

Assuming quasi static (developed) case:

$$q(x=0) = q(x=l)$$

But:

$$q(x=L) = k\,\frac{T - T_o}{L}$$

So:

$$T_o = T_b + \frac{k(T - T_o)}{L\,h}$$

$$T_o + \frac{kT_o}{Lh} = T_b + \frac{kT}{Lh}$$

$$T_o = \frac{T_b + \frac{kT}{Lh}}{1 + \frac{k}{Lh}}$$

$$T - T_o = T - \frac{T_b - \frac{kT}{Lh}}{1 + \frac{k}{Lh}} = \frac{T - T_b}{1 + \frac{k}{Lh}}$$

$$\frac{1}{T - T_o} = \frac{1}{T - T_b}\left(1 + \frac{k}{Lh}\right) = \frac{1}{T - T_b}\left(1 + \frac{1}{Nu}\right)$$

Nusselt Number $\quad Nu = \frac{hL}{k}$

$$\Delta T_{boil} = T_o - T_b = \frac{T_b + \frac{Tk}{Lh}}{1 + \frac{k}{Lh}} - T_b$$

$$\Delta T_{boil} = (T - T_b)\frac{\frac{k}{Lh}}{1 + \frac{k}{Lh}} = \frac{(T - T_b)}{1 + N}$$

3.2.5 From 3.2.3

$$\frac{L}{A}\,\frac{V_m\,\rho_m\,c_m}{(T - T_o)\,k}\,dT = -\,dt$$

ρ_m is a very weak function of T so: $V_m\,\rho_m = m_m$. Taking $1/(T - T_o)$ from 3.2.4:

$$\frac{L}{A}\,m_m\,\frac{c_m(T) * \left[1 + \dfrac{k(T)}{Lh}\right]}{(T - T_b) * k(T)}\,dT = -\,dt$$

Let:

$$y(T) = \frac{c_m(T)\left[1 + \dfrac{k(T)}{Lh}\right]}{(T - T_b) * k(T)}$$

$$\frac{L}{A}\,m_m\,f(T)\,dT = -\,dt$$

Let: $\int_2^{T_{quench}} y(T)\,dT \equiv I_1$ and corresponding Δt_1

$$\int_{2}^{T_{amb}} y(T)\, dT \equiv I_2 \quad \text{and corresponding } \Delta t_2$$

Then:

$$\frac{A}{L} = \frac{m_m * I_1}{\Delta t_1}$$

$$\frac{A}{L} = \frac{m_m * I_2}{\Delta t_2}$$

3.3 Minimal Cross Section Area for Heat Transfer

We get:

$$\frac{L}{A}\, m_m \int_2^{T_{amb}} \frac{c_m \left[1 + \frac{k}{hL}\right]}{(T - T_b)\, k}\, dT = \Delta t$$

The case of:

$$\frac{k}{hL} \gg 1$$

represents one of the following situations:

* $L \to 0$
* k, very big
* h, very small

then:
$$\frac{1 + \frac{k}{hL}}{k} \sim \frac{\frac{k}{hL}}{k} = \frac{1}{hL}$$

and:
$$\frac{m_m}{Ah} \int_2^{T_{amb}} \frac{c_m}{T - T_b}\, dT = \Delta t$$

or:
$$A_{min} = \frac{m_m}{h * \Delta t} \int_2^{T_{amb}} \frac{c_m(T)}{T - T_b}\, dT =$$

$$\frac{m_m}{h * \Delta t} * \text{Int}$$

Assuming that the magnet is represented by properties of copper

$$\int_2^{300} \frac{c_m(T)}{T - 1.4}\, dT = 0.55\ \frac{J}{K}$$

$$A_{min} = \frac{6.5 * 10^5\ g * 0.55\ \frac{J}{K}}{0.02\ \frac{W}{cm^2\ K} * 2.59 * 10^5\ s} = 69\ cm^2$$

3.4 Model Solution

3.4.1 General procedure

a) Assuming L

b) Through 3.2.5 solving (numerically) the integral of f(T) and getting A/L

c) Getting A

d) So, for every L we can find the A

3.4.2 Copper (RRR = 100)

From Table 1 and Fig. 10 we get the y(T) and $\int y(T)\,dt$.

3.4.2.1 L = 5 cm

$$I_1 = \int_2^{120} y(T)\,dT = 2.19\ \frac{s\ cm}{g} \qquad \Delta t_1 = 48\,h = 1.73\ 10^5\ s$$

$$I_2 = \int_2^{300} y(T)\,dT = 5.61\ \frac{s\ cm}{g} \qquad \Delta t_2 = 72\,h = 2.59\ 10^5\ s$$

$$\left(\frac{A}{L}\right)_1 = \frac{m_m\ I_1}{\Delta t_1} = \frac{6.5 * 10^5\,g * 2.19\frac{s\ cm}{g}}{1.73 * 10^5\ s} = 8.23\ cm$$

$$\left(\frac{A}{L}\right)_2 = \frac{m_m I_2}{\Delta t} = \frac{6.5 * 10^5 * 5.61}{2.59 * 10^5} \text{ cm} = 14 \text{ cm}$$

$$A = L\left(\frac{A}{L}\right)_2 = 5 \text{ cm} * 14 \text{ cm} = 70 \text{ cm}^2$$

3.4.2.2 L = 30 cm (Table 1 and Fig. 10)

$$I_1 = 0.456 \frac{\text{s cm}}{G} \qquad I_2 = 0.99 \frac{\text{s cm}}{G}$$

$$\left(\frac{A}{L}\right)_1 = \frac{6.5 * 10^3 * 0.456}{1.73 * 10^5} \text{ cm} = 1.7 \text{ cm}$$

$$\left(\frac{A}{L}\right)_2 = \frac{6.5 * 10^3 * 0.99}{2.59 * 10^5} \text{ cm} = 2.48 \text{ cm}$$

3.4.2.3 L = 60 (Table 1 and Fig. 10)

$$I_2 = 0.54 \frac{\text{s cm}}{g}$$

Table 1: Data and calculations for thermal straps transient analysis.

$h = 0.02 \frac{W}{cm^2 K}$ $T_b = 1.4$ K $y(T) = \frac{c_m \left[1 + \frac{k}{hL}\right]}{(T - T_b)\, k}$ Copper (RRR = 100)

		2	6	10	20	40	60	80	100	120	140	160	180	200	220	260	300
c_m [J g^{-1} K^{-1}]		2.75 10^5	2.28 10^{-4}	8.57 10^{-4}	7.3 10^{-3}	0.059	0.144	0.182	0.255	0.288	0.313	0.332	0.346	0.356	0.356	0.376	0.386
T - T_b [K]		0.6	4.6	8.6	18.6	38.6	58.6	78.6	98.6	118.6	138.6	158.6	178.6	198.6	218.6	258.6	298.6
k [W cm^{-1} K^{-1}]		3	9.5	11	25	15	7.5	5.5	5.0	4.6	4.4	4.2	4.2	4.2	4.2	4.2	4.2
L = 5 cm	1 + k/hL	31	96	111	251	151	76	56	51	47	45	43	43	43	43	43	43
10^4 * y(T) [s cm/g^{-1} k^{-1}]		4.7	5.0	10.1	39.4	153.9	249	235.7	263.8	248.1	231	214.3	198.3	183.5	166.7	148.9	132.3
L = 30 cm	1 + k/hL	6	16.8	19.3	42.7	26	13.5	10.2	9.34	8.7	8.3	8	8	8	8	8	8
10^4 * y(T)		0.91	0.88	1.75	6.7	26.5	44.2	42.8	48.3	46	42.6	39.9	36.9	34.1	31	27.7	24.6
L = 60 cm	1 + k/hL	3.5	8.9	10.2	21.8	13.5	7.25	5.58	5.2	4.83	4.7	4.5	4.5	4.5	4.5	4.5	4.5
10^4 * y(T)		0.53	0.47	0.92	3.42	13.75	23.7	23.4	26.9	25.5	24.1	22.4	20.8	19.2	17.4	15.6	13.8
L = 100 cm	1 + k/hL			6.5	13.5	8.5	4.75	3.25	3.5	3.3	3.2	3.1	3.1	3.1	3.1	3.1	3.1
10^4 * y(T)				0.6	2.2	8.7	15.5	13.6	18.1	17.4	16.4	15.4	14.3	13.2	12	10.7	9.5

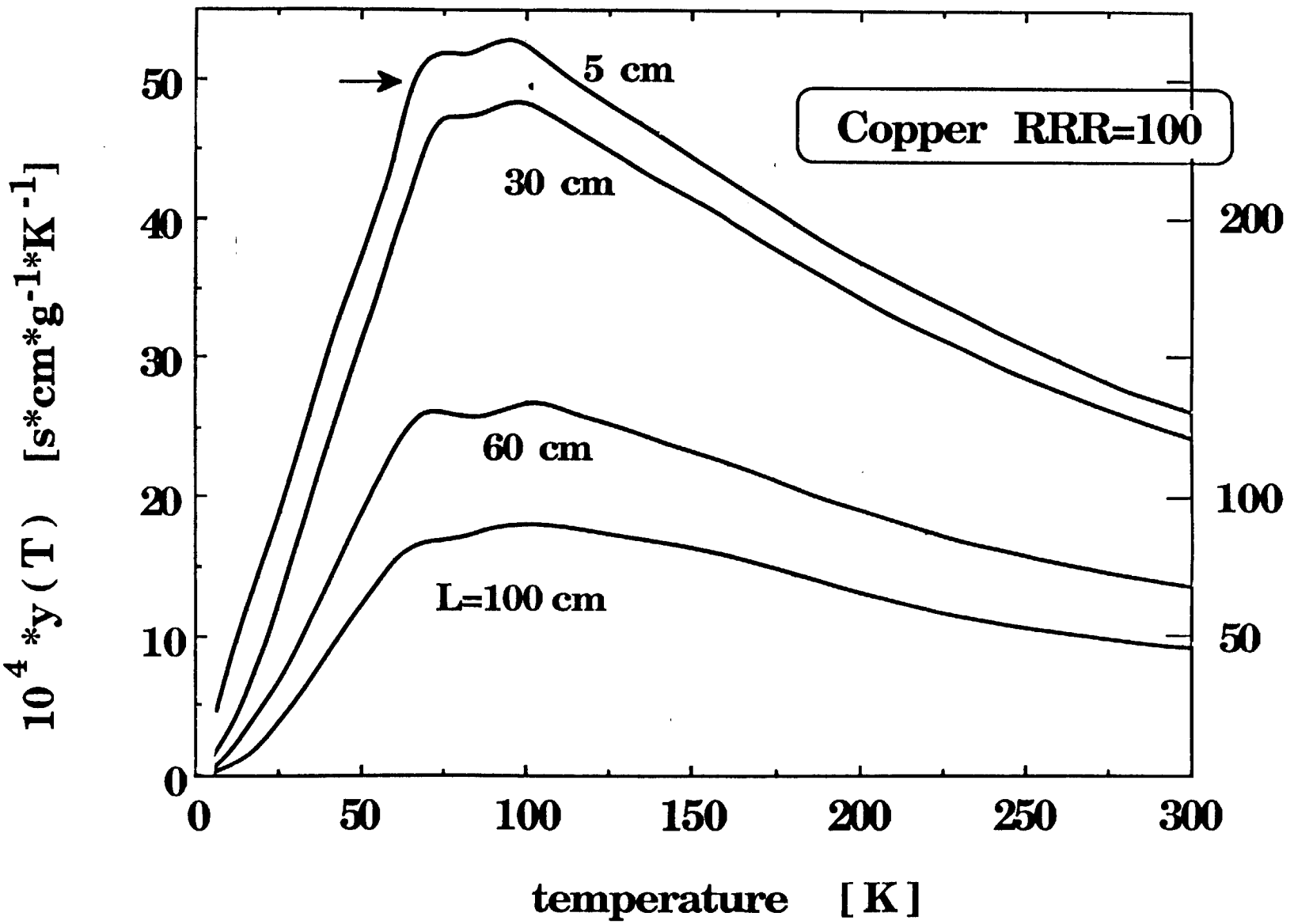

Fig. 10: Copper, $y = \frac{c_m(T)}{k(T)\,(T - T_b)} \left(1 + \frac{k}{hL}\right)$ as function of temperature.

$$\left(\frac{A}{L}\right)_2 = \frac{6.5 * 10^5 * 0.54}{2.59 * 10^5} \text{ cm} = 1.36 \text{ cm}$$

$$A = 60 \text{ cm} * 1.36 \text{ cm} = 81.3 \text{ cm}^2$$

3.4.2.4 L = 100 cm (Table 1, Fig. 10)

$$I_2 = 0.37 \frac{\text{s cm}}{\text{g}}$$

$$\left(\frac{A}{L}\right)_2 = 0.93 \text{ cm}$$

$$A = 100 \text{ cm} * 0.93 \text{ cm} = 93 \text{ cm}$$

3.4.3 Aluminum 5083

3.4.3.1 L = 5 cm (Table 2, Fig. 11)

$$I_2 = 5.9 \frac{\text{s cm}}{\text{g}}$$

$$\left(\frac{A}{L}\right)_2 = \frac{6.5 * 10^5 * 5.9}{2.59 * 10^5} \text{ cm} = 14.8 \text{ cm}$$

$$A = L \left(\frac{A}{L}\right)_2 = 5 \text{ cm} * 14.8 \text{ cm} = 74 \text{ cm}^2$$

3.4.3.2 L = 20 cm (Table 2, Fig. 11)

$$I_2 = 2.02$$

$$\left(\frac{A}{L}\right)_2 = \frac{6.5\ 10^5\ 2.02}{2.59\ 10^5} \text{ cm} = 5.07 \text{ cm}$$

$$A = L \left(\frac{A}{L}\right)_2 = 20 \text{ cm} * 5.07 \text{ cm} = 101.4 \text{ cm}^2$$

3.4.3.3 L = 50 (Table 2, Fig. 11)

$$I_2 = 1.32 \frac{\text{s cm}}{\text{g}}$$

$$\left(\frac{A}{L}\right)_2 = \frac{6.5 * 10^5 * 1.32}{2.59 * 10^5} \text{ cm} = 3.3 \text{ cm}$$

$$A = L\left(\frac{A}{L}\right)_2 = 50 \text{ cm} * 3.3 \text{ cm} = 165 \text{ cm}^2$$

3.4.3.4 L = 80 cm (Table 2, Fig. 11)

$$I_2 = 1.15 \frac{\text{s cm}}{G}$$

$$\left(\frac{A}{L}\right)_2 = 2.8 \text{ cm}$$

$$A = L\left(\frac{A}{L}\right)_2 = 80 \text{ cm} * 2.8 \text{ cm} = 224 \text{ cm}^2$$

Table 2: Data and calculations for thermal straps transient analysis

$h = 0.02 \frac{W}{cm^2 K}$ $T_b = 1.4$ K $y(T) = \frac{c_m \left(1 + \frac{k}{hL}\right)}{(T - T_b)\, k}$ Al-5083

	T [K]	2	4	10	40	80	150	300
	c_m [J g^{-1} K^{-1}]	$2.75\ 10^{-5}$	$9.1\ 10^{-5}$	$8.57\ 10^{-4}$	0.059	0.182	0.322	0.386
	$T - T_b$ [K]	0.6	2.6	8.6	38.6	78.6	148.6	298.6
	k [W cm^{-1} K^{-1}]	0.01	0.03	0.08	0.34	0.56	0.80	1.2
L = 5 cm	1 + k/hL	1.1	1.3	1.8	4.4	6.6	9	13
	10^4 y(T) [s cm g^{-1} K^{-1}]	50.4	15.2	22.4	197.8	273	243.8	140
L = 20 cm	1 + k/hL	1.025	1.075	1.2	1.85	2.4	3	4
	10^4 y(T) [s cm g^{-1} K^{-1}]	47	12.6	14.9	83.2	99.3	81.3	43.1
L = 50 cm	1 + k/hL	1.01	1.03	1.08	1.34	1.56	1.8	2.2
	10^4 y(T)	46.3	12.1	13.41	60.3	64.5	48.8	23.7
L = 80 cm	1 + k/hL	1.006	1.02	1.05	1.21	1.35	1.5	1.75
	10^4 y(T)	46.2	12.0	13.0	54.45	55.8	40.7	18.85

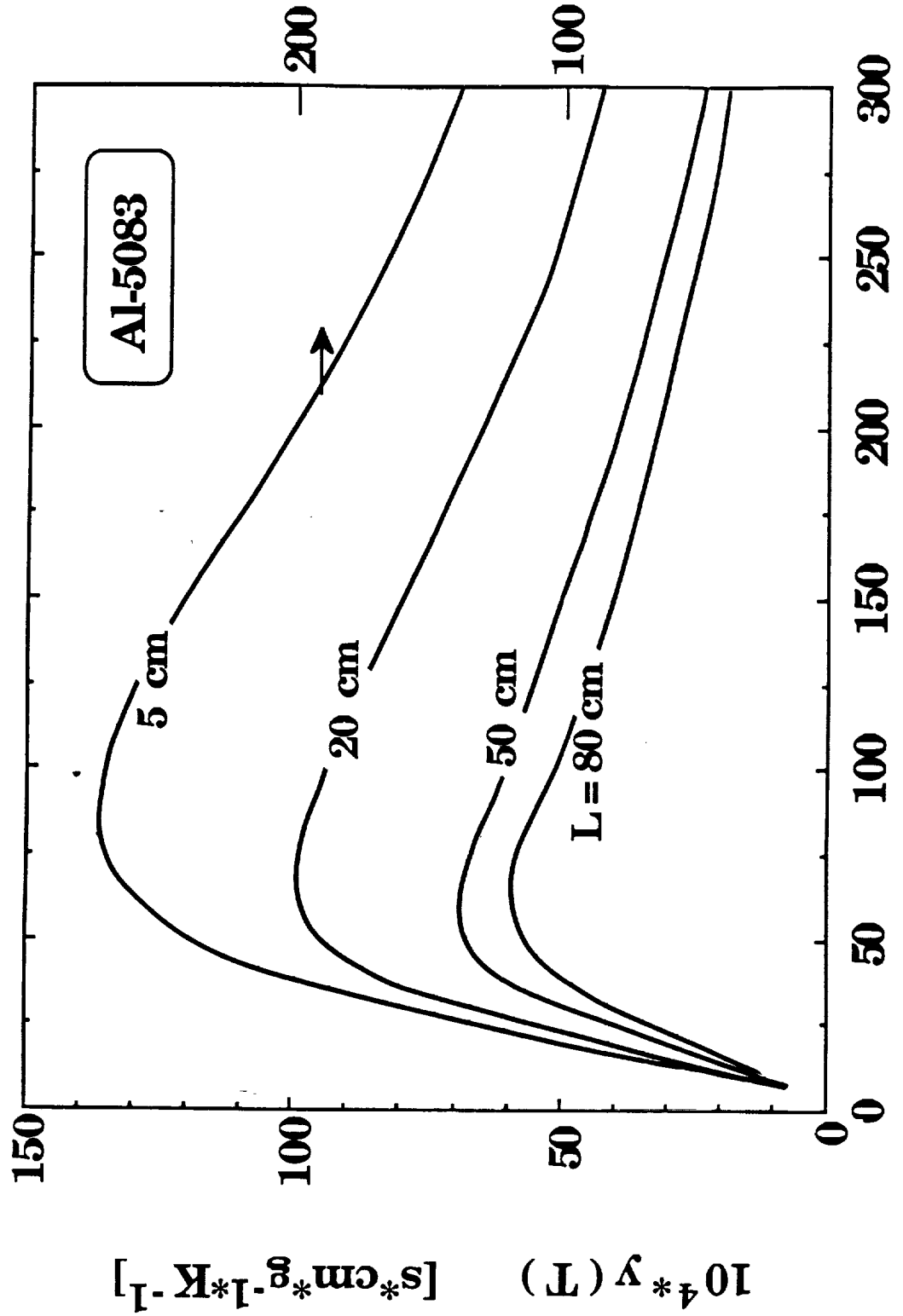

Fig. 11: Aluminum, $y = \frac{c_m(T)}{k(T)\,(T - T_b)} \left(1 + \frac{k}{hL}\right)$ as function of temperature.

3.5 Constant Average Properties Solution

$$\frac{L}{A}\,\frac{c_m\left(1+\frac{k}{hL}\right)}{k}\,\frac{dT}{T-T_b} = -dt$$

$$c_m\,(T) \rightarrow c_{av}$$

$$k\,(T) \rightarrow k_{av}$$

$$\frac{L}{A}\,\frac{c_{av}\left(1+\frac{k_{av}}{hL}\right)}{k_{av}}\,\frac{dT}{T-T_b} = -dt$$

$$\frac{L}{A}\,\frac{C_{av}\left(1+\frac{k_{av}}{hL}\right)}{k_{av}} \equiv \Delta\,\tau$$

$$\frac{dT}{T-T_b} = -\frac{dt}{\tau}$$

$$\ln (T - T_b)\Big|_2^T = \frac{t}{\tau}$$

$$\ln \frac{T - T_b}{2 - T_b} = \frac{t}{\tau}$$

$$T_b = 1.4 \qquad \ln \frac{T - 1.4}{0.6} = \frac{t}{\tau}$$

3.6 Magnet Temperature Decrease as Function of Time

Figure 12 shows the general behavior of the relative cooling down time as function of the temperature for different cases.

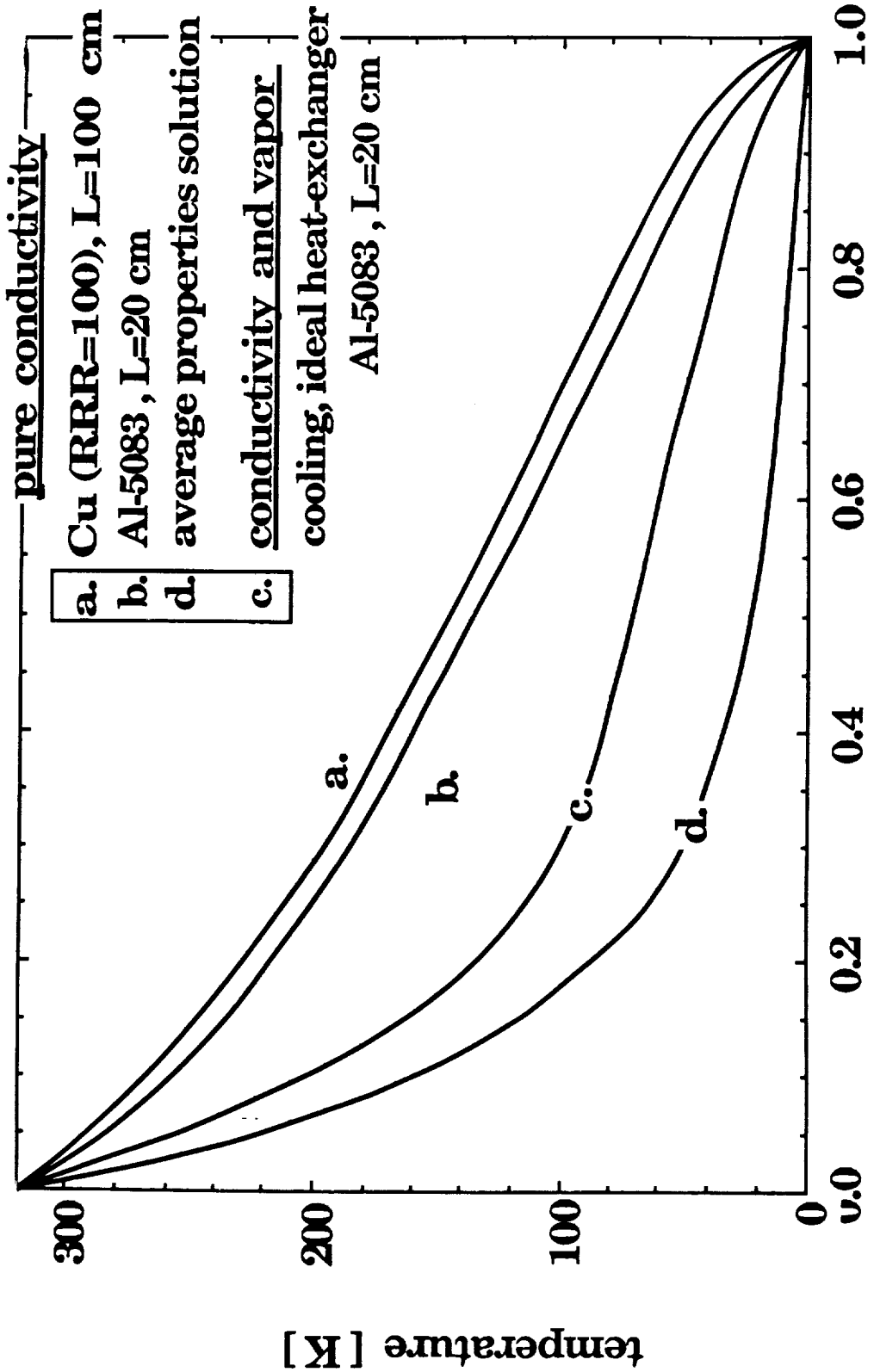

Fig. 12: Temperature reduction while magnet cooling down.

3.7 Starp's Cold End Temperature

3.7.1 General

In 3.2.4 we have seen:

$$T - T_o = \frac{T - T_b}{1 + \frac{k}{hL}}$$

So

$$T_o = T - \frac{T - T_b}{1 + \frac{k}{hL}} = \frac{T\,\frac{k}{hL} - T_b}{1 + \frac{k}{hL}}$$

3.7.2 Copper

3.7.2.1 L = 5 cm

T (K)	20	40	100	160	200	260	300
T_o (K)	19.9	39.7	98	156.2	195.3	254	293
$T - T_o$	0.1	0.3	2	3.8	4.7	6	7

3.7.2.2 L = 60 cm

T (K)	20	40	100	160	200	260	300
T_o (K)	18.1	36.9	80.5	124.1	155.2	201.9	233
$T - T_o$	1.9	3.1	19.5	35.9	44.8	58.1	67

3.7.3 Al 5083 L = 50 cm

T (K)	10	40	80	150	300
T_o (K)	1.3	9.4	27.8	65.9	163
$T - T_o$	8.7	30.6	52.2	84.1	137

Figure 13 shows T_o and $T - T_o$ for each T.

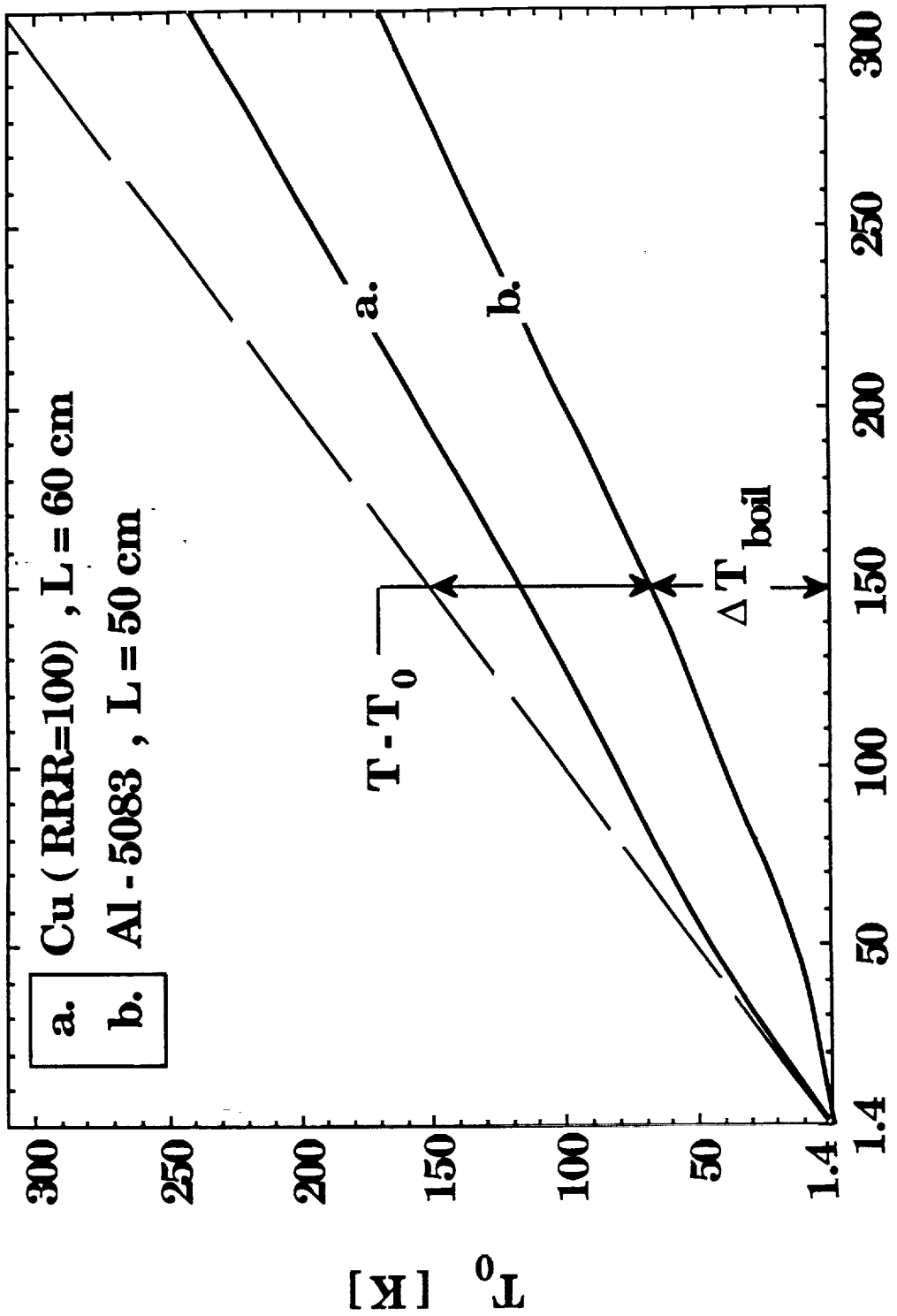

Fig. 13: Thermal strap cold end temperature while magnet cooling down, as function of magnet's temperature.

3.8 Heat Power

3.8.1 General

The highest heat flux occurs at the first instant of cooling down, T = 300 K

$$q = -k \frac{dT}{dx} \qquad \dot{Q} = kA \frac{dT}{dx}$$

approximated through our model as:

$$\dot{Q} = k\, A \frac{T - T_o}{L} = k \frac{A}{L} (T - T_o)$$

$$\dot{Q}_{peak} = k * \frac{A}{L} (T_{amb} - T_o)$$

3.8.2 Copper RRR = 100

3.8.2.1 L = 5 cm

$$\frac{A}{L} = 14.0 \text{ cm} \qquad T_{amb} - T_o = 7 \text{ K}$$

$$\dot{Q}_{peak} = 4.2 \frac{W}{cm\ K} * 14 \text{ cm} * 7 \text{ K} = 412 \text{ W}$$

From Chapter 3.1.6: $\dot{Q}_{av} = 100.4$ W

$$\frac{\dot{Q}_{peak}}{\dot{Q}_{av}} = 4.1$$

3.8.2.2 L = 60 cm

$$\frac{A}{L} = 1.36 \text{ cm} \qquad T_{amb} - T_o = 67$$

$$\dot{Q}_{peak} = 4.2 * 1.36 * 67 \text{ W} = 382.7 \text{ W}$$

$$\frac{\dot{Q}_{peak}}{\dot{Q}_{av}} = 3.8$$

3.8.3 Al 5083 L = 50 cm

$$\frac{A}{L} = 3.3 \text{ cm} \qquad T_{amb} - T_o = 137 \text{ K}$$

$$\dot{Q}_{peak} = 1.2 \frac{W}{cm\ K} 3.3 \text{ cm} * 137 \text{ K} = 542.5 \text{ W}$$

$$\frac{\dot{Q}_{peak}}{\dot{Q}_{av}} = 542.5 / 100.4 = 5.4$$

3.9 Model Evaluation

3.9.1 Exact integral solution

The model ensures removal of the exact total internal energy.

3.9.2 The model uses to some extent higher heat fluxes than the real ones. So to some extent it underestimates the real cooling down time.

3.9.3 It better approximates the cooling range from 300 K to 120 K. In that range the thermal conductivity is almost temperature independent. So a longer portion of the temp. profile is linear.

3.9.4 The ratio of maximal heat power to the average one is about 5, which seems acceptable.

4. TRANSIENT ANALYSIS: COOLING DOWN THROUGH CONDUCTION AND VAPOR

4.1 Shortage of Sole Strap Conduction Cooling Down

After quench the internal energy of 11 MJ has to be removed. That is equivalent to the magnet stored energy. The latent heat of evaporation for He II:

$$\lambda \cong 20 \text{ J/G}$$

So the required amount of He II for recovery would be:

$$\frac{11 \text{ MJ}}{20 \text{ J/g}} = 5.5 * 10^5 \text{ G} = 550 \text{ kg}$$

equivalent to 3850 dcm^3. That is about half of the intended tank's volume.

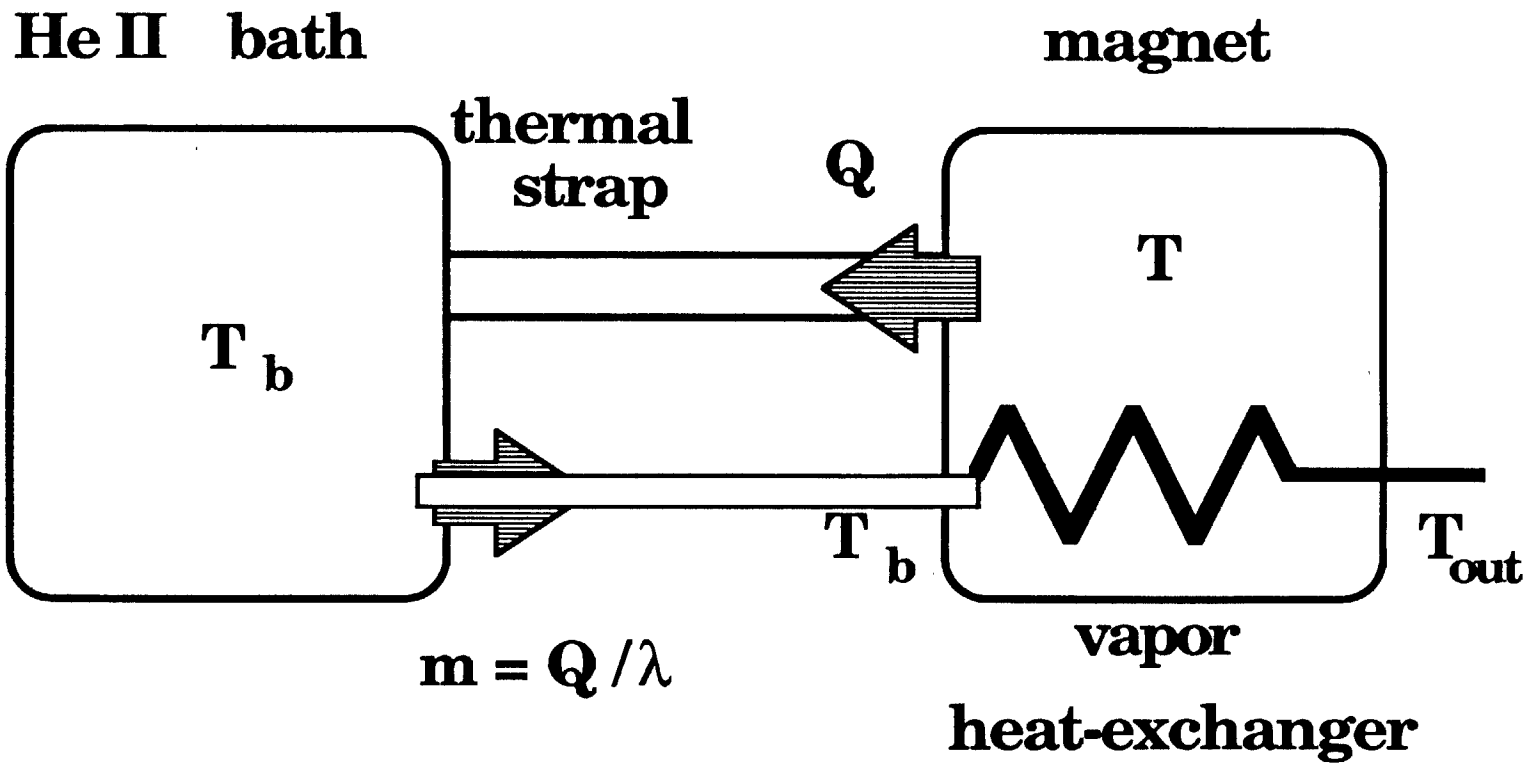

Fig. 14: Layout and notation of magnet cooling down by thermal strap and vapor heat exchanger.

4.2 Additional Cooling by Vapor

By passing the boiled off vapor through the magnet more energy is subtracted from every unit of He II. Instead of utilizing only the latent heat before releasing the vapor it enables additional cooling by convection. Schematically it is described in Fig. 14.

Vapor is generated according to the amount of heat transported through thermal strap to helium bath (dewar). That vapor cools the magnet while flowing through it. In the inlet vapor's temperature is that of the helium bath and at the outlet, T_{out}, according to the efficiency of the heat exchanger.

4.3 Short Heat Exchanger Case

4.3.1 Mathematical model

$$m_m\, c_m \frac{dT}{dt} = -k \frac{dT}{dx} A_s - h\, A_v\, (T - T_b)$$

where A_s, cross section of conducting strap,

A_v, area of heat convection from magnet to vapor,

T_b, bath or vapor temp.

Similarly to the transient model the dT/dx is approximated by $(T - T_o)/L$

$$m_m\, c_m \frac{dT}{dt} + \frac{k\, A_s}{L} (T - T_o) + h\, A_v\, (T - T_b) = 0$$

$$T - T_o = \frac{T - T_b}{1 + \frac{k}{hL}}$$

Assuming that the thermal conductance, h, is the same at the boiling film on the cold end of the strap and between magnet and vapor

$$m_m c_m \frac{dT}{dt} + \frac{k A_s}{L} \frac{T - T_b}{1 + \frac{k}{hL}} + h A_v (T - T_b) = 0$$

$$m_m c_m \frac{dT}{dt} = - \frac{k h A_s}{hL + k} (T - T_b) - h A_v (T - T_b)$$

$$m_m c_m \frac{dT}{dt} = \frac{h A_s}{1 + \frac{hL}{K}} (T - T_b) - h A_v (T - T_b)$$

$$m_m \frac{c_m}{(T - T_b)\left[\frac{A_s}{1 + \frac{hL}{k}} + A_v\right] h} dT = - dt$$

It can be integrated similarly to the case of transient solution (without vapor) because the left wing is but temperature dependent.

4.3.2 Minimal convection and conduction areas

$$\frac{m_m\, c_m}{h\,(T - T_b)\left[\dfrac{A_s}{1 + \dfrac{hL}{k}} + A_v\right]}\, dT = -\, dt$$

For $L \to 0$ or for $k \to \infty$ we get:

$$\frac{m_m}{h}\,\frac{c_m}{(T - T_b)}\,\frac{dT}{A_s + A_v} = -\, dt$$

$$(A_s + A_v)_{min} = \frac{m_m}{h * \Delta t}\int \frac{c_m\, dT}{T - T_b} \equiv \frac{m_m}{h * \Delta t} * \text{Int}$$

That integral was calculated in 3.3.1, so that

$$(A_s + A_v)_{min} = 69\ cm^2$$

For $A_v/A_s = 1$

$$A_s = A_v = 34.5\ cm^2$$

4.3.3 Solution (example)

Instead of integration we might have an approximate solution based on the previous transient case integration (without vapor cooling). Rearranging the diff. equ. to:

$$\frac{L}{A_s}\, m_m\, \frac{c_m\left(1 + \frac{k}{hL}\right)}{(T - T_b)\, k}\, \frac{1}{1 + \left(1 + \frac{hL}{k}\right)\frac{A_v}{A_s}}\, dT = -dt$$

$$\text{Let: } Z = \frac{1}{1 + \left(1 + \frac{hL}{k}\right)\frac{A_v}{A_s}}$$

The present solution differs from the previous one by Z.

Assumptions

4.3.3.1 For copper RRR = 100 or Al RRR = 1500 or other high conductance material, for L < 100 cm, h = 0.02 W/cm K

$$\frac{hL}{k} \ll 1$$

4.3.3.2 For Al 5083 and L = 20 cm on average along the whole temperature range

$$\frac{hL}{k} \sim 0.3$$

4.3.3.3

$$\frac{A_v}{A_s} = \text{Const}$$

4.3.4 Results

1. For high k materials $Z = \dfrac{1}{1 + \dfrac{A_v}{A_s}}$

2. For Al 5083 and L = 20 cm $Z = \dfrac{1}{1 + 1.3\,\dfrac{A_v}{A_s}}$

3. The solving integral is proportional to the integral in the case of sole conduction. Denoting:

$$\int_{2}^{T_{amb}} \frac{c_m \left(1 + \frac{k}{hL}\right)}{(T - T_b)\, k} \frac{1}{1 + \left(1 + \frac{hL}{k}\right)\frac{A_v}{A_s}}\, dT \equiv (II)_1$$

So:

$$(II)_2 = \frac{I_2}{Z}$$

and

$$\frac{A_s}{L} = \frac{m_m}{\Delta t}\,(II)_2 = \frac{m_m}{\Delta t}\,\frac{I_2}{Z}$$

4.3.4.1 Assuming $A_v/A_s = 1$ that:

for case 4.3.3.1 Z = 0.50 and

for case 4.3.3.2 Z = 0.43

To sum up:

4.3.4.2 For copper RRR = 100, Al RRR = 1000 and k/Lh >> 1

L = 30 cm $A_s = 37.2$ cm $= A_v$

L = 60 cm $A_s = 40.8 \text{ cm} = A_v$

L = 100 cm $A_s = 46.5 \text{ cm} = A_v$

4.3.4.3 For Al 5083

L = 20 cm $A_s = 43.6 \text{ cm}^2 = A_v$

4.3.5 Reduction in boil off while cooling down

The parameter Z represents the ration between the heat flux in case of sole conduction and the case of conduction plus vapor cooling.

Under the above assumptions, when Z is constant, it means that the fluxes are proportional at every moment to those of the case of cooling through thermal strap only.

Therefore the total amount of energy removed through conduction in presence of vapor cooling is lower by the factor Z.

The boil off is reduced by the factor Z.

4.4 Ideal Heat Exchanger

The vapor passes through a heat exchanger in the magnet. It's outlet temperature reaches the temperature T of the magnet.

$$m_m\, c_m \frac{dT}{dt} = -\dot{m}\, c_p\, (T - T_b) - \frac{k\, A}{L}\, (T - T_o)$$

$\dot{m}$, helium vapor mass flow rate

c_p, helium vapor heat capacity

$$\dot{m} = \dot{Q}_{strap} / \lambda$$

$\dot{Q}_{strap}$, heat power transferred through straps

λ, latent heat of evaporation

$$\dot{Q}_{strap} = \frac{k\, A}{L}\, (T - T_o)$$

Through chapter 4.3.1:

$$\dot{m} = \frac{k\, A}{\lambda\, L}\, \frac{T - T_b}{1 + \frac{k}{hL}}$$

$$m_m\, c_m\, \frac{dT}{dt} = -\frac{k\, A\, c_p}{\lambda\, L\left(1 + \frac{k}{hL}\right)}\,(T - T_b)^2 - \frac{A}{L}\,\frac{k}{1 + \frac{k}{hL}}\,(T - T_b)$$

$$\frac{L}{A} = m_m\,\frac{c_m}{\frac{k\, c_p}{\lambda\left(1 + \frac{k}{hL}\right)}\,(T - T_b)^2 + \frac{k}{\left(1 + \frac{k}{hL}\right)}\,(T - T_b)}$$

$$g(T) = \frac{c_m}{\frac{k\, c_p}{\lambda\left(1 + \frac{k}{hL}\right)}\,(T - T_b)^2 + \frac{k}{1 + \frac{k}{hL}}\,(T - T_b)}$$

for Al 5083 L = 20 cm according to Table 3 and Fig. 15.

$$I_2 = 0.12\ \frac{s\ cm}{g}$$

$$\frac{A}{L} = \frac{6.5 * 10^5 * 0.12}{2.59 * 10^5} = 0.30\ cm$$

$$A = 20\ cm * 0.15\ cm = 3\ cm^2$$

Table 3: Data and calculations for thermal strap and ideal heat exchanger transient analysis.

λ = 22 J/g $h = 0.02 \frac{W}{cm^2 K}$ L = 20 cm Al-5083

T (K)	2	4	10	40	80	150	300
c_m [J g^{-1} K^{-1}]	$2.75 * 10^{-5}$	$9.1 * 10^{-5}$	$8.57 * 10^{-4}$	0.059	0.182	0.322	0.386
T - T_b [K]	0.6	2.6	8.6	38.6	78.6	148.6	298.6
k [W cm^{-1} K]	0.01	0.03	0.08	0.34	0.56	0.80	1.2
1 + k/(hL)	1.025	1.075	1.2	1.85	2.4	3	4
c_p [J g^{-1} K^{-1}]	5.24	4.08	5.41	5.20	5.2	5.2	5.2
k c_p/λ [W cm^{-1} K^{-2}]	$2.38 * 10^{-3}$	$5.56 * 10^{-3}$	0.0196	0.08	0.132	0.189	0.283
k / (1 + k/hL)	0.0097	0.028	0.067	0.183	0.233	0.267	0.3
10^4 g(T) [s cm $g^{-1}K^{-1}$]	0.413	8.44	4.80	8.25	5.08	2.25	0.6

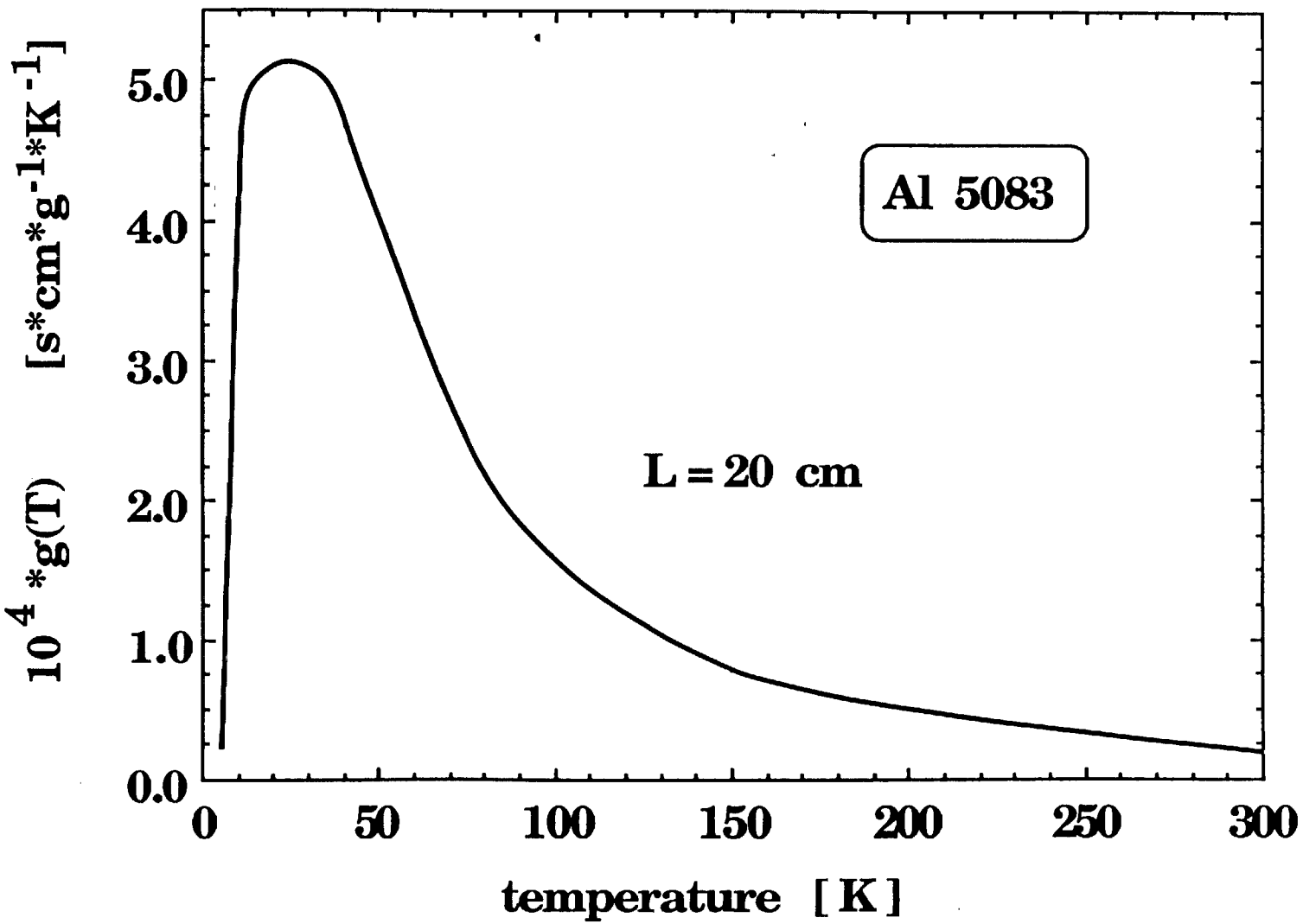

Fig. 15: Aluminum, $g = \frac{c_m}{\frac{k c_p}{\lambda}(T - T_b)^2 + \frac{k h L}{K + hL}(T - T_b)}$ as function of T.

The peak heat flux through thermal strap:

$$\dot{Q}_{peak} = k\ A\ \frac{T_{amb} - T_o}{L} = \frac{A}{L}\ \frac{k}{1 + \frac{k}{hL}}\ (T_{amb} - T_b)$$

$$= 0.3\ cm * 0.3\ \frac{W}{cm\ K}\ (300\ K - 1.4\ K) = 26.9\ W$$

Through chapter 3.1.6 we have seen:

$$\dot{Q}_{av} = 100.4\ W$$

or

$$\frac{\dot{Q}_{peak}}{\dot{Q}_{av}} = \frac{26.9}{100.4} = 0.26$$

We might wish to compare the peak heat flux through the thermal strap to the case of sole strap cooling (without vapor) for Al 5083 L = 50 cm which is 2.5 times longer than the present strap (with vapor cooling) we got in chapter 3.8.3.

$$\frac{\dot{Q}_{peak}}{\dot{Q}_{av}} = 5.4$$

Put another way, the peak heat flux is reduced by a factor of 5.4/0.26 = 20.7. It means that the perfect heat exchanger is making the major cooling work. However, the thermal straps are essential to transport heat for vapor generation.

4.5 Real heat exchanger

$$m_m * c_m \frac{dT}{dt} = - kA \frac{T - T_o}{L} - \dot{Q}_{HX}$$

The rate of heat transfer in a real heat exchanger, $\dot{Q}_{HX}$, is ruled[ ] by the logarithmic average of temperature differences:

$$\dot{Q}_{HX} = U * A_v * \frac{\Delta T_c - \Delta T_w}{\ln \frac{\Delta T_c}{\Delta T_w}}$$

$$\Delta T_c = T - T_b$$

$$\Delta T_w = T - T_{out}$$

$$\dot{Q}_{HX} = U * A_v \frac{T_{out} - T_b}{\ln \frac{T - T_b}{T - T_{out}}} \qquad (4.5.1)$$

Energy balance on vapor stream

$$\dot{m} * c_p (T_{out} - T_b) = \dot{Q}_{HX} = U * A_v \frac{T_{out} - T_b}{\ln \frac{T - T_b}{T - T_{out}}}$$

$$\ln \frac{T - T_b}{T - T_{out}} = \frac{U A_v}{\dot{m} * c_p} \qquad (4.5.2)$$

Vapor's flowrate derives from heat power conducted to the bath through the thermal strap:

$$\dot{m} \lambda = A * k \frac{T - T_o}{L}$$

Through chapter 4.3.1

$$\dot{m} = \frac{A * k}{\lambda L} \frac{T - T_b}{1 + \frac{k}{hL}} \qquad (4.5.3)$$

The overall balance differential equation:

$$m_m * c_p * \frac{dT}{dt} + \frac{kA}{L\left(1 + \frac{k}{hL}\right)} (T - T_b) + U * A_v \frac{T_{out} - T_b}{\ln \frac{T - T_b}{T - T_{out}}} = 0 \qquad (4.5.4)$$

In its final form the model consists of:

(a) differential equation:

$$\frac{dT}{dt} = - \frac{kA}{m_m * c_p * L\left(1 + \frac{k}{hL}\right)} (T - T_b)\left[1 + \frac{c_p}{\lambda}(T_{out} - T_b)\right] = 0$$

(b) transcendental equation:

$$\ln \frac{T - T_b}{T - T_{out}} = \frac{U * \lambda * L}{c_p * k} \frac{A_v}{A} \frac{\left(1 + \frac{k}{hL}\right)}{(T - T_b)}$$

Well approximated:

$$U = h$$

Through the transcendental equation (b) T_{out} is solved as function of T. Then equation (a) is integrated to get T(t).

5. THERMAL STRAP SUMMARY: CONCLUSIONS AND DESIGN REMARKS

5.1 The constraints derived from steady state analysis and from transient analysis are plotted for Al 5083 on Fig. 16 and for Cu RRR = 100 on Fig. 17.

5.2 The steady state constraints are much more restrictive, so they should dominate the design.

5.3 For a steady state mixed case

$$R = \frac{L_1}{k_1 A_1} + \frac{L_2}{k_2 A_2} + \frac{1}{h_c A_3} + \frac{1}{h_b A_1} < \frac{\Delta T}{\dot{Q}}$$

R, thermal resistance

h_c, contact heat transfer coefficient (A_3)

h_b, boiling heat transfer coefficient (A_1)

5.4 As a general trend increasing A_v enables reducing the A_s for a desired after quench boil of amount.

5.5 Because of the domination of the steady state case, we may avoid the transient analysis for the mixed case (different material for strap).

5.6 The contact conductance between the metal seems to be significant so the contact areas are suggested to be enlarged.

5.7 Using high purity metal (high conduction and high elongation) in between structural ends (low conduction and stiff) seems to be a mechanical advantage. It enables self adjustment, lower tolerances and easier assembly.

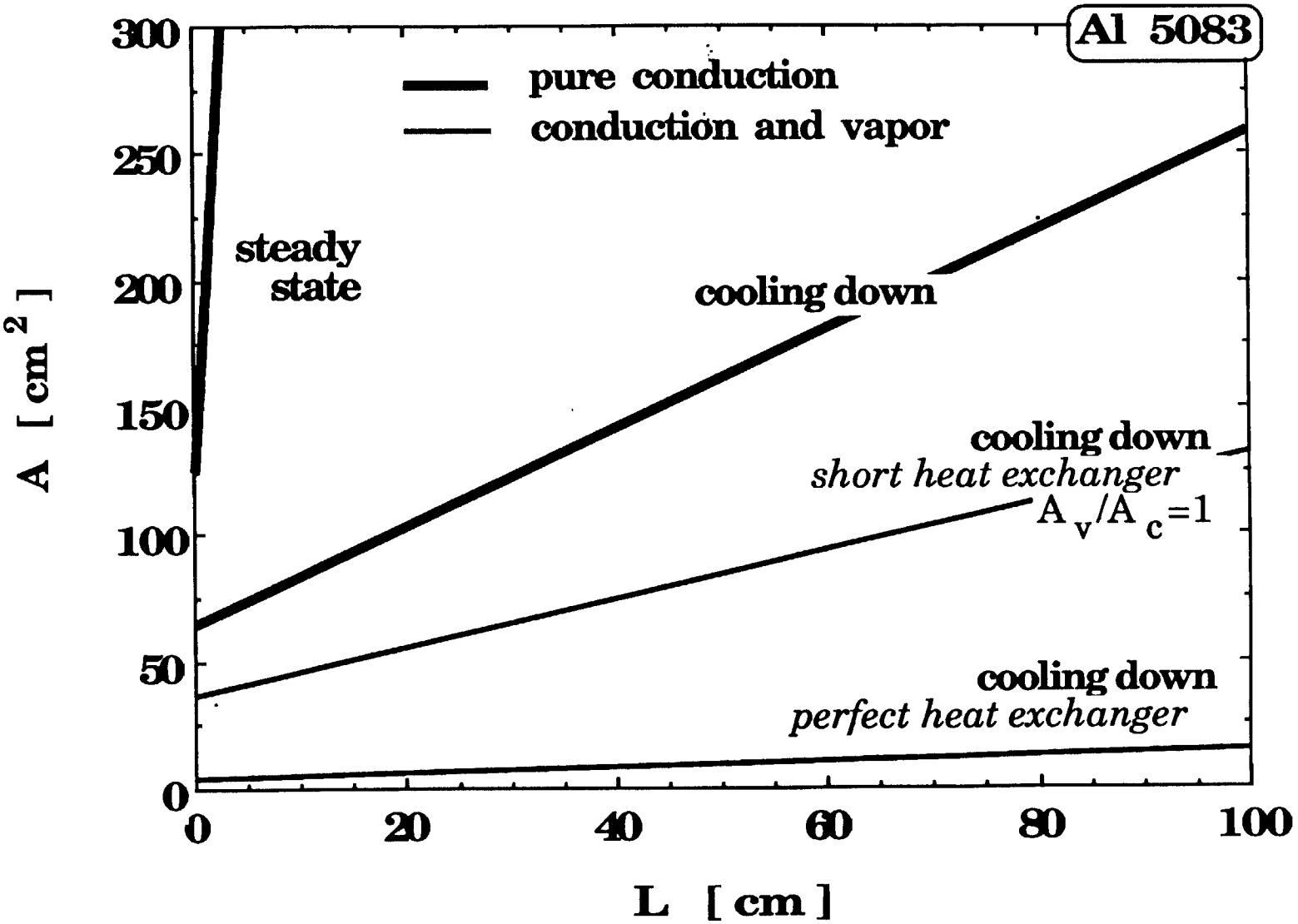

Fig. 16: Restrictive sizing characteristics of aluminum thermal strap at various modes of operation.

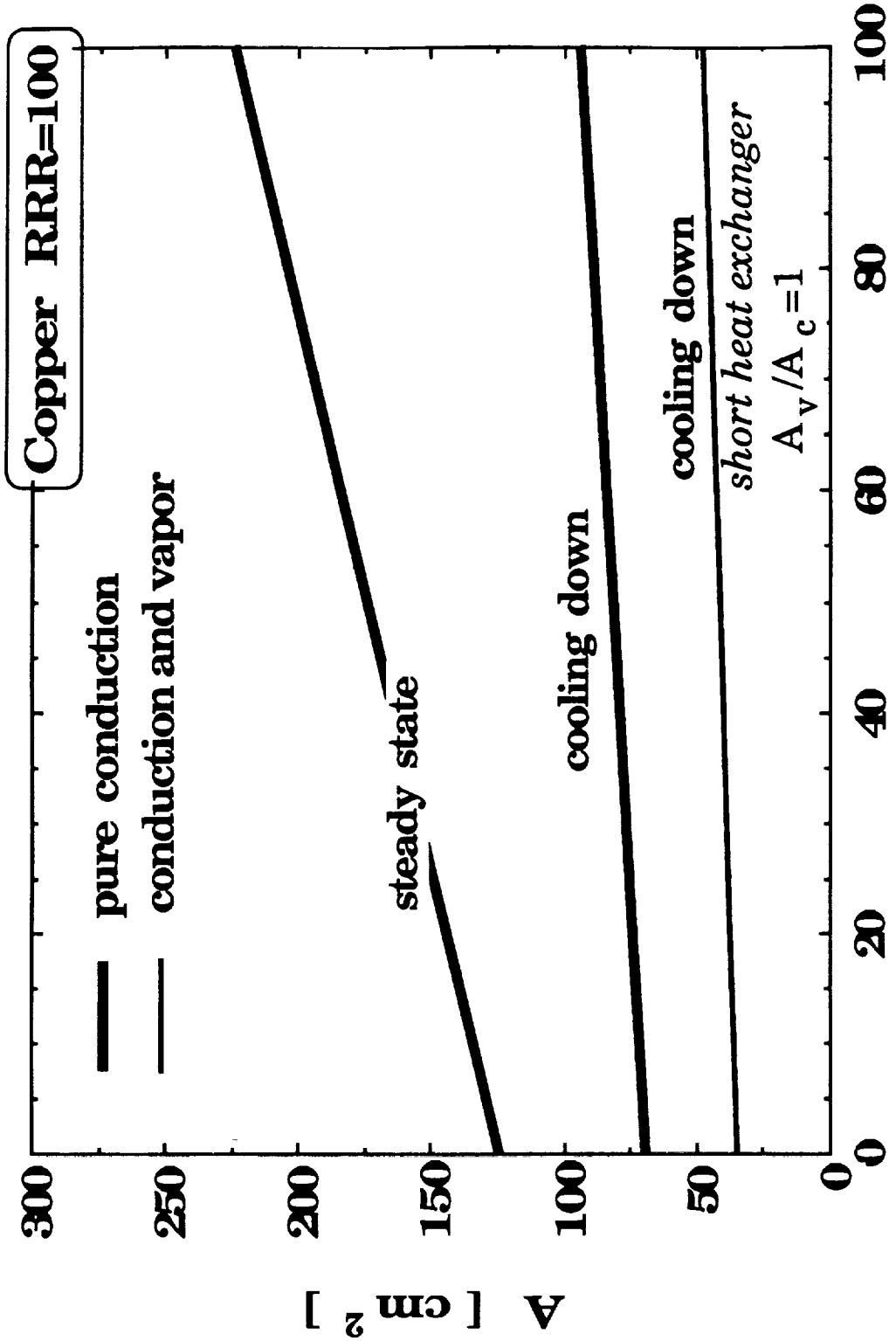

Fig. 17: Restrictive sizing characteristics of copper thermal strap at various modes of operation.

6. PRELIMINARY DESIGN ATTEMPT

6.1 Principles

6.1.1 To meet the general layout and interfacing according to source 2 (Fig. 1, p. 3).

6.1.2 In order to shorten the cold end of the strap (being made of low conductive, construction alloy) it will be part of the dewar design.

6.1.3 Contact area enlargement

6.1.4 Using Al RRR = 1500

6.1.5 Vapor heat transfer area if considered as the whole magnet surface.

$$A_v = 166 \text{ cm} * \pi * 18.4 \text{ cm} = 9590 \text{ cm}^2$$

6.2 Sizing

D = 166 cm

δ (contact) = 10 cm	δ (conduction) = 2 cm
Al 5083	H.P. Al
L = 2 cm + 2 cm	L = 20 cm

$A_s = 166 \text{ cm} * 3.14 * 2 \text{ cm} = 1043 \text{ cm}^2$

$A_{contact} = 5220 \text{ cm}^2$

6.3 Conduction

$$R = \frac{4}{0.015\ 1043} + \frac{20}{5\ 1043} + \frac{2}{0.005\ 5220} + \frac{1}{0.02\ 5220}$$

Al 5083 H.P. Al contacts film boiling.

$$R = 0.255 + 0.004 + 0.076 + 0.01 = 0.345\ \frac{K}{W}$$

$$\Delta T = R\ \dot{Q} = 0.25\ W * 0.345\ \frac{K}{W} = 0.08\ K < \underline{0.1\ K}$$

6.4 Vapor Cooling

$$R_v = \frac{1}{h_b\ A_v} = \frac{1}{0.02 * 9590} = 0.052\ \frac{K}{W}$$

$$\frac{R}{R_v} = \frac{0.345}{0.052} = 6.63$$

6.5 Thermal Stresses

To ensure that the developed thermal stresses in strap between 300 K and 1.5 K will not cause failure.

The elongation for H.P. Al (to failure) is about 30%. The thermal expansion in our case is

$$\frac{L_{293} - L_0}{L_{273}} = 415\ 10^{-5} = 0.415\ \%$$

It seems to be able to withstand the tensile stresses.

There is no problem of buckling since the stresses are tensile.

Derived general layout shown in Fig. 18.

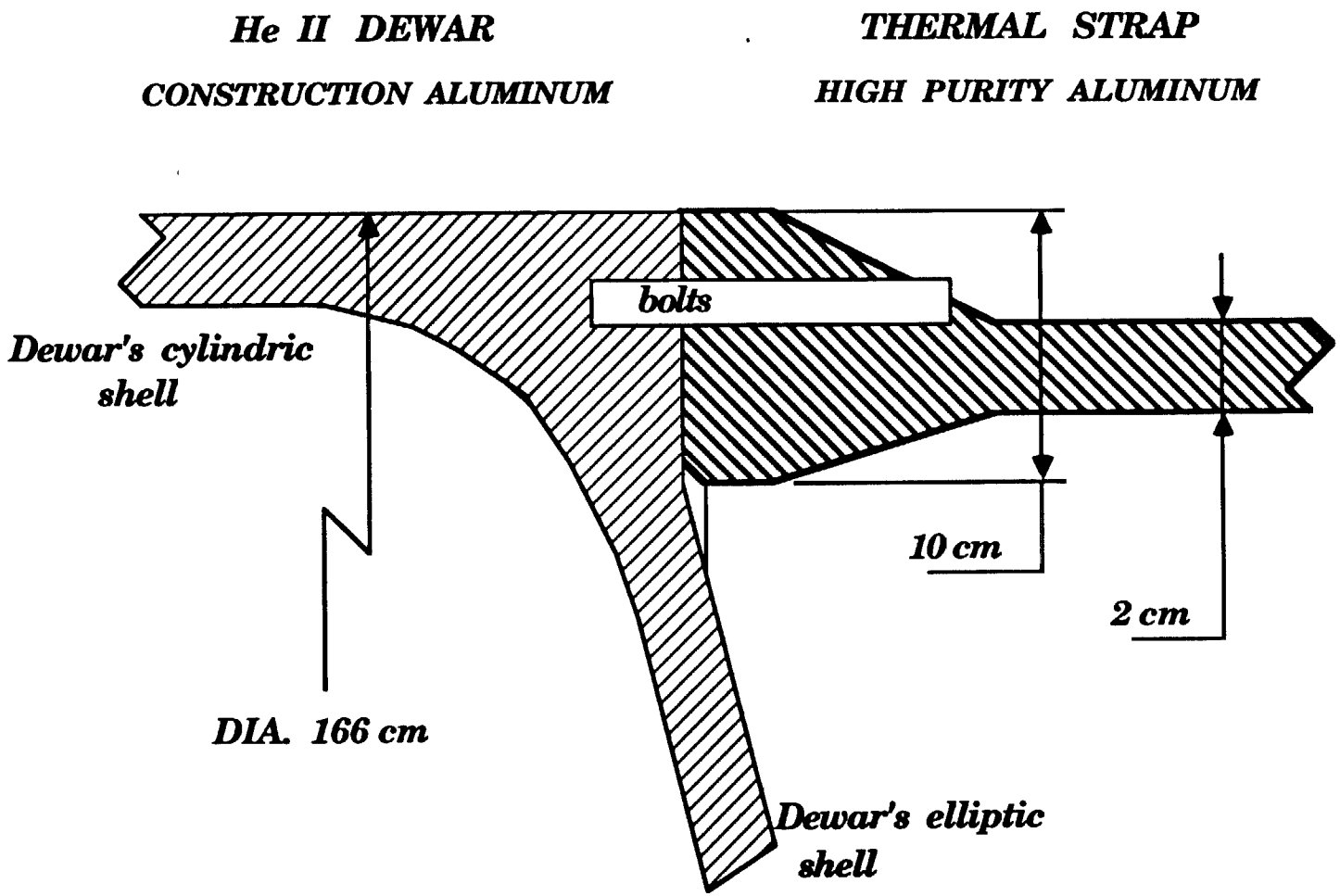

Fig. 18: Preliminary design attempt of a thermal strap.

7. HE II INTERNAL CONVECTION COOLING SYSTEM

7.1 Introduction

Many space-based low temperature systems use stored He II (T < 2.2 K) to supply cooling. Included among these are infrared telescopes such as IRAS, COBE and SIRTF, as well as specialized systems like ASTROMAG, a particle physics experiment. In all cases, these cryogenic systems require a thermal link between the liquid helium dewar and the principal low temperature device, i.e., telescope or superconducting magnet. A number of possible approaches exist to make this thermal link. In the case of infrared telescopes, the main approach has involved direct thermal contact through support structure or high conductivity thermal straps. This method has been successfully applied to the IRAS and COBE cryogenic system. By contrast, the ASTROMAG cryogenic system has a leading design which involves the use of a self-activated fountain effect pumping system. The use of He II in direct contact with the superconducting magnets may be desirable because of the need to ensure a higher degree of thermal stabilization.

In the present chapter we consider an alternative approach for cooling large He II cryogenic systems in zero-gravity. This approach involves the use of a kind of heat pipe which relies on counterflow heat transport in the He II contained in channels linking the dewar to the low temperature device. If it could be made to work effectively, a He II heat pipe system would provide better thermal contact than the high thermal conductivity straps. It also may be simpler to implement

and more reliable than the self-activating fountain effect pump.

The self-activating fountain effect pumping system (Hofmann loop) has been the preferred concept for cooling of the superconducting magnets in ASTROMAG.[7] The device uses a fountain pump activated by the parasitic heat leak into the magnet to force the He II to circulate through tubes surrounding the magnet.[14] Fountain pumps have been developed for space-based systems as part of the Superfluid Helium On-Orbit Transfer (SHOOT) demonstration. Advantages include simplicity of design, where the pump consists of a heater and porous ceramic plug, and the tendency to suppress cavitation, a problem more common in centrifugal pumps with He II. The principal disadvantage, that of a low thermodynamic efficiency, is overcome in the Hofmann loop by relying on the heat leak into the system to drive the pump.

7.2 He II Internal Versus External Convection

To consider whether the Hofmann loop makes sense for ASTROMAG, one must compare the relative merits, mostly improved cooling, with the increased complexity associated with the added components (pumps, heat exchangers and flowmeters) in the cryogenic system. Some of these issues require more detailed design; however, scaling arguments can be used for comparison. One issue to consider is whether the forced circulation will result in any benefit to heat exchange between the magnet and He II reservoir. Two factors are important here. First, the heat exchange process between the surface of the cooling channel and the He II is not affected by flow rate. This fact, which has been demonstrated experimentally[19,20], results from the surface heat transfer being dominated by Kapitza conductance. Kapitza conductance is a phonon-mediated process which is not affected by the relatively small velocities of He II forced flow.

Forced flow can have a significant impact on the heat transport in bulk He II. However, the question remains as to whether this process is of benefit to the ASTROMAG cooling system. One can determine the temperature profile in forced flow He II by analysis of the steady state He II energy equation

$$\frac{d}{dx}\left[\left(\frac{1}{f}\frac{dT}{dx}\right)^{1/3}\right] - \rho\, c\, v\frac{dT}{dx} + \frac{dq_{gen}}{dx} = 0 \qquad (7.1)$$

where $f = A\,\rho_n/\rho_s^3\,s^4\,T^3$, the He II thermal resistance parameter with A being the Gorter-Mellink mutual friction parameter. Solution to eq. (7.1) depends on the particular boundary conditions; however, it is possible to show by dimensionless scaling that the parameter

$$K = \rho\, c_p\, v\, (fL)^{1/3}\, \Delta T^{2/3} \tag{7.2}$$

provides a measure of the degree to which heat is carried by forced convection compared to internal convection. If $K' > 1$, there will be a significant increase over static internal convection. Two variables in eq. (2) which must be determined are the fluid velocity and temperature rise ΔT in the helium.

The He II flow rate through the system is determined by the performance of the fountain effect pump. For an ideal pump working against negligible pressure head the mass flow is given by

$$\dot{m} = \frac{\dot{Q}}{s_{in}\, T_{in}} \tag{7.3}$$

For a 10 mW heat generation at 1.4 K, eq. (7.3) yields a corresponding mass flow rate of about 50 mg/s. This mass flow rate results in a pressure drop through the hydraulic circuit. In turbulent flow, it has been shown that pressure drop in He II can be analyzed in terms of classical friction factor correlations.[21] For the sake of

simplicity, we assume that the Blasius correlation is appropriate for describing the friction factor and the pressure drop can be given by

$$\Delta p = 4 f_D \frac{L}{D} \left(\frac{1}{2} \rho v^2 \right) \tag{7.4}$$

where $f_D = 0.079/Re^{1/4}$, which is appropriate for Reynolds numbers in the range 10^4. Substituting for the friction factor and rewriting in terms of mass flow rate, we obtain

$$\Delta p = 0.241 \frac{L}{D^{19/4}} \frac{\eta_n^{1/4}}{\rho} \left(\frac{Q}{sT} \right)^{7/4} \tag{7.5}$$

The magnitude of the temperature change ΔT can be estimated by consideration of the fountain pump. If we assume that the pump has ideal behavior, then London's equation applies, $\Delta p = \rho s \Delta T$. The corresponding temperature difference is that which must be maintained across the pump to produce the required mass flow rate. This may not be the highest temperature in the flow loop, but it would be expected to be close except possibly at very high mass flow rates. Combining London's equation with eq. (7.5) yields,

$$\Delta T = 0.241 \frac{L}{D^{19/4}} \frac{\eta_n^{1/4}}{\rho^2 s} \left(\frac{Q}{sT} \right)^{7/4} \tag{7.6}$$

As an example, for a 10 mW heat generation at 1.4 K with L = 30 m and D = 7 mm, eq. (7.7) predicts a temperature rise across the circuit of about 50 μK, while 250 mW would result in $\Delta T \sim 14$ mK.

To determine the relative importance of forced convection heat transfer, we can compute the value of K′ by substituting eq. (7.6) and (7.3) into (7.2). The result is

$$K = 0.493 \frac{Q^{13/6} c_p f^{1/3} L \eta_n^{1/6}}{D^{31/6} \rho^{4/3} s^{17/6} T^{13/6}} \tag{7.7}$$

As an example, for a 10 mW heat leak at 1.4 K and for ASTROMAG cooling loop geometry, eq. (7.7) predicts a $K' \sim 5 \times 10^{-4}$. During charge when Q = 250 mW, we obtain $K' \sim 0.5$. Note also that if the temperature increases, the value of K′ further decreases because of the strong temperature dependence to the entropy.

7.3 He II Heat Pipe System

The above result that forced convection contributes little to the heat transport in an ASTROMAG cooling loop except under extraordinary conditions calls into question the use of a self-activated fountain pump system in this application. The enhancement of cooling is small and the added complexity of design significant. Therefore, it seems appropriate to consider alternative cooling schemes for this system. One option is to use a simple static cooling loop which relies on internal convection to remove the steady state heat generation. We refer to this device as a He II Heat Pipe. Such a cooling system could be equipped with a fountain pump which would operate only for emergency conditions such as recovery from quench.

A schematic representation of a He II Heat Pipe system for ASTROMAG is shown in Fig. 19. The magnet is indirectly cooled by a loop containing static He II. Each end of the loop penetrates the main helium dewar. Porous plugs located at the loop ends are needed to ensure that the helium within the cooling loop remains above saturation pressure. The dewar must also contain fluid acquisition devices (FAD) so that the porous plugs will be in continuous contact with He II. The loop is equipped with a heater (H) and bypass valve (BV) to allow the porous plug to function as a fountain pump under extraordinary operation such as magnet cooldown or recovery from a quench.

There are two primary issues which must be considered when designing a He II

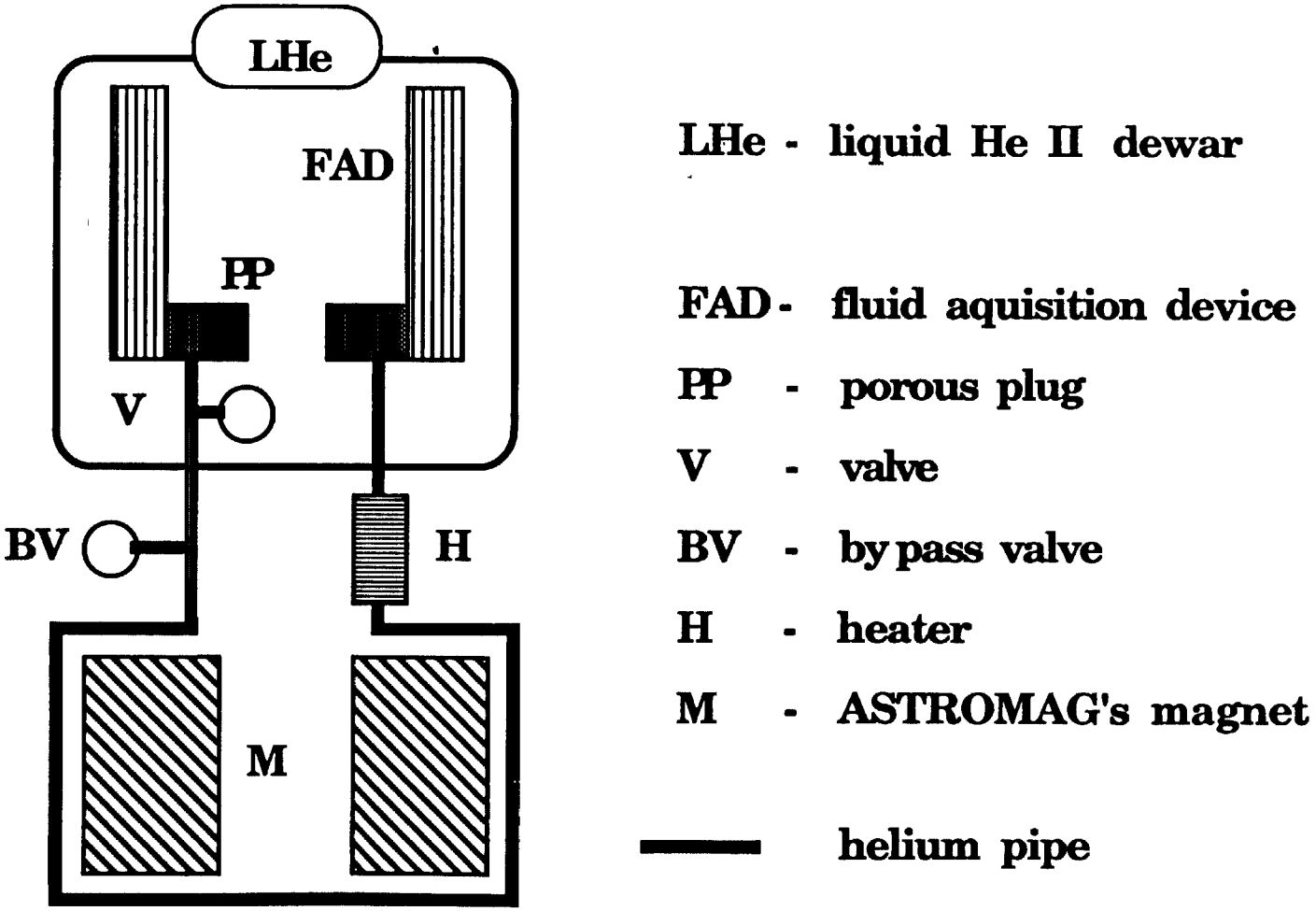

Fig. 19: Schematic representation of He II Heat Pipe system for ASTROMAG.

Heat Pipe system. These are that the loop must have sufficient cooling capability to remove the expected heat leak and that the helium within the loop must not cavitate. The heat removal capability of a cooling loop is determined by its physical dimensions and the allowable temperature difference within the system. This problem can be analyzed by knowing the total heat load on the loop and applying the heat transport equations appropriate for He II.

7.4 Temperature Drops Along the Heat Pipe

For the purpose of analysis, we assume that the cooling loop consists of a one-dimensional channel of length L and diameter D, which receives a heat load $\dot{Q}$ distributed uniformly along its length. The loop is terminated at both ends by porous plugs, where we model as large number, N, of parallel capillaries of length l and diameter d. The channel diameter and heat flux within the helium is taken to be large enough to obey turbulent heat transport so that the temperature gradient is given by

$$\frac{dT}{dx} = f\, q^3 \tag{7.8}$$

where q is the heat flux W/cm^2. For a channel of length L with constant temperature boundary conditions, the temperature difference between the middle and ends can be obtained by integration of eq. (7.8) to yield,

$$\Delta T_1 = \left(\frac{Q}{\pi D^2}\right)^3 f\, L \tag{7.9}$$

For typical ASTROMAG parameters, Q = 10 mW, D = 7 mm, L = 30 m and for T = 1.8 K, $f \cong 10^{-13}\ m^5\ K/W^3$, then $\Delta T_1 \sim 1\ \mu K$. Even under extraordinary conditions with Q = 250 mW the temperature difference is 13 mK, a generally small value.

The temperature difference across the porous plug is more complex owing to the normal fluid drag which contributes to the loss mechanism. Assuming that the porous plug can be modeled as N parallel capillaries, the temperature gradient is given by

$$\frac{dT}{dx} = \frac{\beta \eta_n q}{(\rho s d)^2 T} + f q^3 \qquad (7.10)$$

The first term on RHS is the normal fluid drag. The normal fluid viscosity is η_n and β is a geometrical factor which depends on channel geometry but is 32 for circular cross-section. For a porous plug of a given porosity, $\sigma = N\pi d^2/4A_p$, and length l, the temperature difference across it, ΔT_2, may be calculated by integrating eq. (7.10).

$$\Delta T_2 = \frac{g}{d^2}\left(\frac{Q}{\sigma A_p}\right) l + f\left(\frac{Q}{\sigma A_p}\right)^3 l \qquad (7.11)$$

where we define $g \equiv \beta \eta_n/(\rho s)^2 T$, the laminar flow thermal resistivity function. Note that $g \sim T^{-12}$ so its contribution to the overall temperature difference depends strongly on the operating temperature range. Under most conditions of operation for ASTROMAG, the first term in eq. (7.11) will dominate the temperature difference across the plug. However, depending on the choice of pore diameter,

the turbulent term may have a significant effect.

An approximate numerical estimate for the contribution that the porous plug makes to the overall heat removal of the He II heat pipe can be obtained by inserting typical values in eq. (7.11). At 1.8 K, $g \sim 4 \times 10^{-15}$ Km^3/W. For a steady heat leak of 10 mW, d = 10 μm, σ = 0.5, l = 1 cm and A_p = 0.4 cm^2, we obtain ΔT_2 = 0.18 mK. Even for extraordinary conditions with Q = 250 mW, $\Delta T_2 \sim 5$ mK, an acceptable value. A summary of different operating conditions and pore sizes are listed in Table 4.

7.5 Porous Media Evaluation

The main purpose of the porous plug is to provide a pressure head so that the fluid within the channel will not cavitate when it receives a modest temperature rise due to heat exchange. In laminar flow, the pressure gradient is the result of normal fluid drag and can be written

$$\frac{dp}{dx} = \frac{\beta \eta_n v_n}{d^2} \tag{7.12}$$

where v_n is the normal fluid velocity. Equation (7.12) is simply the Poiseuille expression for the normal fluid component. In counterflow, $v_n = q/\rho sT$. Further, the pressure and temperature gradients are simply related through London's equation. If we model the porous plug as a number of channels of length l diameter d undergoing laminar flow, then the above equations can be integrated to establish the size of the pressure difference across the plug for a given heat flux.

Above the critical velocity, London's equation is no longer valid owing to the onset of turbulence in the fluid. The effect of turbulence is largest in the temperature gradient because of the existence of the mutual friction term, second term in eq. (7.10). In some treatments of pressure gradient in counterflow He II, there is a second non-linear term which adds to eq. (12) such that

$$\frac{dp}{dx} = \frac{\beta \eta_n v_n}{d^2} + 0.00494 \left[\mathrm{Re}(v_n)\right]^{1.75} \qquad (7.13)$$

which is appropriate for Re > 1200. Since the contribution by the second term is only significant for relatively high velocities, we will neglect it here and treat the temperature gradient explicitly in terms of eq. (7.12). This is the so called Allan-Reekie Rule.

The situation we encounter with respect to the porous plug operation in reduced gravity is best described in terms of the liquid helium phase diagram, Fig. 20. We assume that the helium within the storage dewar is at saturation, thus being represented by a point b with a bath temperature T_2. The helium within the heat pipe will be at a higher temperature, T_1, as a result of heat absorbed from the residual heat leaks or charging losses to the magnet. If the porous plug behaved as an ideal fountain pump then the pressure difference would be given by London's equation, which corresponds to a process of constant chemical potential, μ = const. The pressure in the loop would be given by point a′, which is well above saturation and therefore would prevent cavitation. Without the porous plug, there would be no significant fountain pressure produced, because the channel diameter is too large. In this case, the pressure within the heat pipe would be given by point b′, which is within the vapor region of the phase diagram

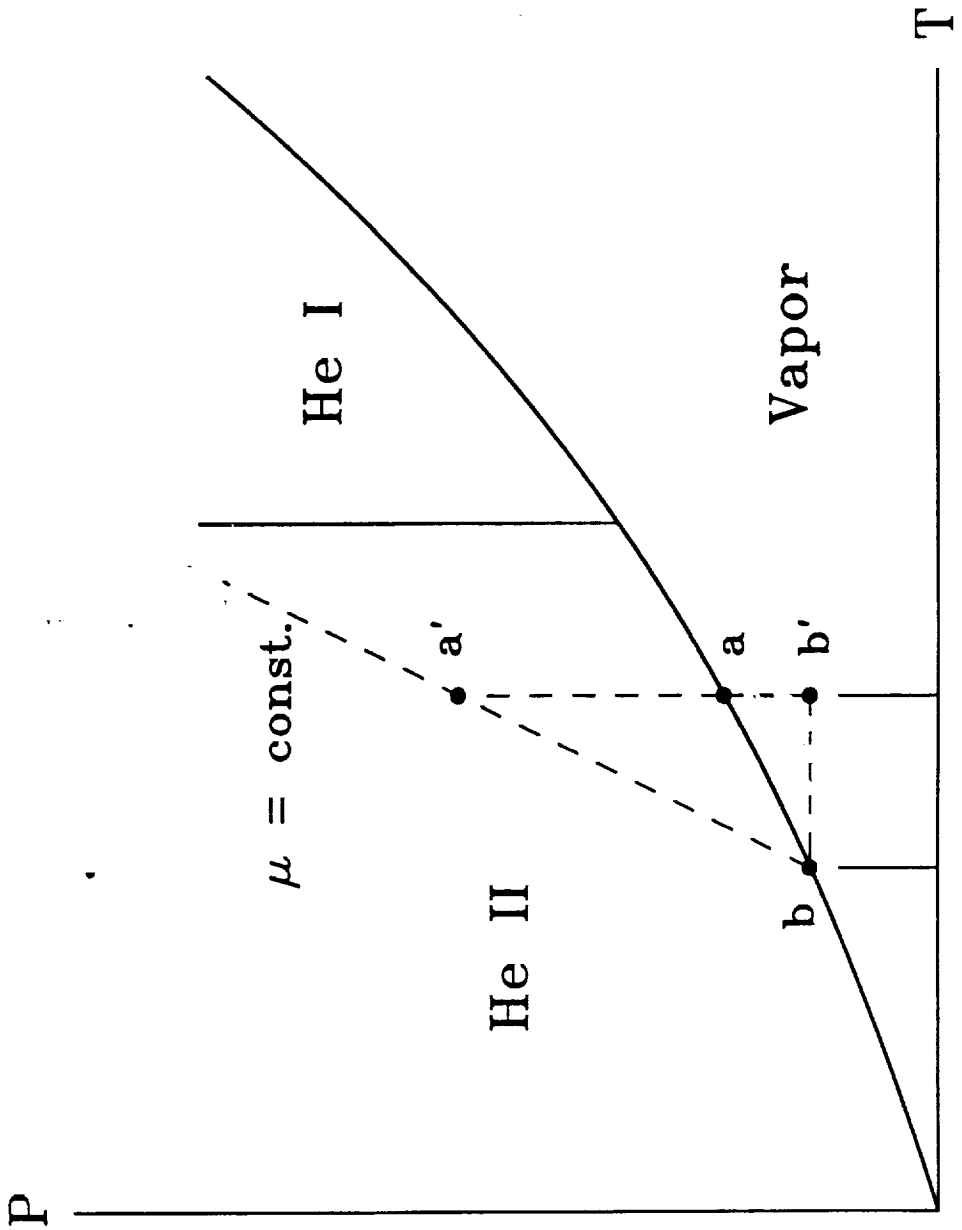

Fig. 20: Porous plug operation described in terms of liquid helium phase diagram.

and would result in cavitation and vapor lock of the loop.

A third possibility is to have the porous plug present at the terminations of the loop, but to have larger pores so that there is some fountain pressure achieved but it is not as large as predicted by London's equation. The advantage of larger pores is in the plugs' improved ability to transport heat from the loop to the storage dewar. The important characteristic of the intermediate pore size model is to ensure that the pressure rise, due to the fountain effect, be larger than the slope of the vapor pressure curve,

$$\left(\frac{dP}{dT}\right)_{fe} > \left(\frac{dP}{dT}\right)_{svp} \tag{7.14}$$

Combining eqs. (10) and (12), we get that

$$\left(\frac{dP}{dT}\right)_{fe} = \frac{\rho s}{1 + \frac{fd^2}{g} q^2} \tag{7.15}$$

Also, using the Clausius-Clapeyron equation and assuming ideal gas behavior we get

$$\left(\frac{dp}{dT}\right)_{svp} \cong \frac{\lambda}{T v_g} \sim \frac{\lambda p}{RT^2} \tag{7.16}$$

where λ is the latent heat of helium and v_g is the specific volume of the vapor. The above two equations can be combined to get the conditions in heat flux and pore diameter in the plug

$$qd < \left[\frac{g}{f}\left(\frac{\rho s\, RT^2}{\lambda p} - 1\right)\right]^{1/2} \tag{7.17}$$

Inserting values for ASTROMAG at 1.8 K, q = 500 W/m^2 requires that d < 1.3 mm which is quite large for porous media. On the other hand, during charging, the heat flux will increase by a factor of 25 which would therefore require d < 50 μm. Listed in Table 5 are the maximum diameters for a variety of operating conditions and temperature as calculated from eq. (7.17). To ensure sufficient heat removal and safe non-cavitating operation of the heat pipe, the plug should have a pore size around 10 μm. It also would be advantageous to fabricate the plug of a high conductivity metal, such as copper, to enhance the heat exchange between the helium within the loop and the bath.

The use of a He II heat pipe for cooling of ASTROMAG would seem to be justified

based on the above arguments. As envisioned, the system would consist of a cooling loop containing static He II terminated by porous plugs immersed in the storage dewar. Steady state and charging heat leaks could easily be removed by this system. However, the question remains as to the behavior of the system during extraordinary operation such as initial cooldown or magnet quench. These modes of operation will require active control.

First, consider the behavior of the He II heat pipe during magnet quench. One of the most important issues here is to minimize the loss of helium inventory. Since the He II heat pipe contains relatively little helium of its own (approximately 10 liters), this helium would need to vent due to rapid vaporization. Relief values (RV) are required for this purpose (see Fig. 19). Subsequent to the quench, the magnet is expected to be at relatively high temperatures (100 - 120 K). Cooldown and resupply would therefore be accomplished by opening the vent valve to space. This process would allow helium to circulate through the loop. Initially, the loop would be filled with low pressure vapor, thus cooling would be rather slow. In fact, the porous plug might act as a phase separator in this situation preventing the liquid from entering the loop. To ensure rapid cooldown, the porous plug would need to be equipped with a heater to keep the downstream temperature above that of the helium within the storage dewar, thus activating the fountain effect. Helium would be circulated through the loop until the magnet is returned to operating temperature. Initially, the helium would vent, but subsequently,

when He II is being circulated. Opening of v_2 would allow recovery of the helium to the storage dewar. A similar procedure would apply when cooling the magnet from initial ambient temperature.

Using the porous plug as a fountain pump should be straightforward since the porous plug is intended to establish a significant fountain pressure during steady state operation. However, because of the need to extract heat through the plug, it would not be expected to operate as an ideal fountain pump. Even for an ideal pump, the mass flow rate is reduced below that given by eq. (7.3) as the result of hydrodynamic pressure loss. In general, the mass flow rate is given by[13]

$$\dot{m} = \frac{\dot{Q}}{6.6 \frac{\Delta p}{\rho} + s_{in} T_{in}} \tag{7.18}$$

For high mass flow rates such as are required for SHOOT or may be required for ASTROMAG during extraordinary operation do result in sizable pressure drops and therefore reduced mass flow rates. Also, because of the heat leak due to normal fluid flow through the porous plug, the heat required to achieve a given $\dot{m}$ would be larger than predicted by eq. (7.18).

7.6 Conclusion

A He II heat pipe based on the principals described in this report should work effectively for heat removal from the magnets for ASTROMAG. The primary heat exchange mechanism would be that of internal convection. As envisioned, the heat pipe would consist of a tube wrapped around the magnet having either end terminate within the helium storage dewar. Each end of the tube has a porous plug which serves to prevent cavitation while at the same time allowing heat transfer. Based on preliminary calculations, a plug having the same cross-section as the tube but consisting of multibore tubes of diameter 10 μm should perform adequately. Further analysis and experimentation would be required to verify these findings.

Table 4. Temperature difference across a 1 cm long plug for different hole diameters and heat fluxes. A_p = 0.4 cm^2, Q = 10 mW or 250 mW.

q (W/m^2) d (micro m)	500 1	500 10	12500 1	12500 10
Temp (K)	Δt (K)	ΔT (K)	ΔT (K)	ΔT (K)
1.4	0.431	0.00431	10.83	0.155
1.5	0.174	0.00174	4.379	0.060
1.6	0.076	0.00076	1.912	0.026
1.7	0.035	0.00035	0.902	0.012
1.8	0.018	0.00018	0.452	0.006
1.9	0.009	0.00009	0.242	0.003
2	0.005	0.00005	0.138	0.003
2.1	0.003	0.00003	0.103	0.008

Table 5. Maximum pore diameter to prevent cavitation. A_p = 0.4 cm^2; Q = 10 mW and 250 mW, σ = 0.5.

	q (W/m^2)	500	12500
Temp (K)	p (Pa)	max d (mm)	max d (mm)
1.4	282	1.256	0.050
1.5	472	1.340	0.053
1.6	746	1.407	0.056
1.7	1128	1.434	0.057
1.8	1638	1.382	0.055
1.9	2299	1.204	0.048
2	3129	0.858	0.034
2.1	4141	0.359	0.014

8. HOFMANN'S LOOP SYSTEM

8.1 Introduction

The central idea of Hofmann's Loop System (HLS) is to use object's anyway dissipated heat for driving a Fountain Effect Pump (FEP) and sustain an external convection He II cooling system. Furthermore, one might expect it to be a self-sustained cooling loop in the sense of feedback system which means: a transient increase in heat load will drive stronger the FEP, increase the flowrate and its cooling capacity. Decrease in dissipation will affect in the opposite direction. It was suggested and analyzed theoretically in source (14) and checked through a lab model as summarized in sources (15), (16) and (17).

However, some difficulties arise while trying to apply that idea for cooling the ASTROMAG. In the previous chapter (7) a comparison was drawn between internal and external convection. Since the HLS is one of the leading design concepts the following chapter is a more detailed attempt to derive its main parameters to meet the ASTROMAG's cooling and performance specifications[2,3] for demonstrating its shortages.

8.2 Non-Dissipated Heat Load

While the dissipated energy of the magnet is used to drive the FEP, part of it "is saved" from being dissipated as mechanical work. It is the work for circulating

the He II fluid and does not account as boil-off.

However, an idealized analysis based on perfect heat exchangers (14) shows that the maximum energy porition saved and converted to mechanical work does not exceed 10%. That is consistent with a result obtained in (13) saying that the maximum efficiency of a FEP is about 15%.

Practically, with non-ideal heat exchangers one should expect about 5% of the dissipation saved as mechanical work.

8.3 Flow Velocity and Mass Flowrate

Matching the ASTROMAG steady state requirements was demonstrated in previous chapters through conduction of thermal straps. The equivalent thermal conduction of He II (or its internal convection) is higher by about two orders of magnitude than that of any metal. So, just the internal convection is adequate for the steady state cooling. Therefore, the criteria for minimal HLS velocity is suggested: the heat transport through convection should be about twice the conductive heat transport. Put another way the total heat transport is required to be about 3 times the conductive (internal convection) heat transport.

Van Sciver[11] showed for small ΔT that external and internal heat transport relation is ruled by a non-dimensional parameter K, defined as:

$$K = \rho * c_p * V * (fL)^{1/3} (T_m - T_b)^{2/3}$$

where: v - velocity

f - temperature dependent He II heat conductivity function (source)

L - channel length

$T_m - T_b$ - temperature difference across the channel

To match the above criteria for minimal HLS velocity, the non-dimensional parameter K has to reach the value of 5.

$T = 1.4 \div 1.5$ K

$\rho = 0.14$ G $\cdot$ cm^{-3}

$c_p \cong 1$ J $\cdot$ g^{-1} $\cdot$ K^{-1}

$f(T) \cong 1/300$ cm^5 $\cdot$ K $\cdot$ W^{-3}

$T_m - T_b \cong 0.3$ K

$K = 5$

According to source (3) the length of the channel might be 20 to 40 m and its diameter 6 to 8 mm.

For: L = 20 m and D = 8 mm.

$$v = \frac{K}{\rho * c_p (fL)^{1/3} (T_m - T_b)^{2/3}} =$$

$$= \frac{5}{0.14 \frac{g}{cm^3} * 1 \frac{J}{g*K} * \left(\frac{1}{300} \frac{cm^5 * K}{W^3} * 2000\,cm \right)^{1/3} 0.3^{2/3} * K^{2/3}}$$

$$= 42.3 \frac{cm}{s}$$

The mass flowrate:

$$\dot{m} = \rho * v * A$$

$$D = 0.8\ cm$$

$$\dot{m} = 0.14 \frac{g}{cm^3} * 0.64\ cm^2 * 42.3 \frac{cm}{s} = 3.8 \frac{g}{s}$$

if D = 0.6 cm then $\dot{m}$ = 2.14 g/s

For L = 40 m and D = 0.6 cm

$$v = 33.6 \frac{cm}{s}$$

$$\dot{m} = 1.7 \frac{g}{s}$$

For L = 30 m and D = 0.6 cm

$$v = 37.0 \frac{cm}{s}$$

$$\dot{m} = 1.86 \frac{g}{s}$$

8.4 FEP's Driving Heat Power

The interaction of a FEP and a transfer line was formulated and solved in source (13). Following that procedure some heat powers and pressure drops are derived for L = 20, 30, 40 m and D = 6, 8 mm, T = 1.4, 1.5 K. For small velocities f is approximated as 0.004 to simplify the calculations.

8.4.1 L = 20 m T = 1.4 K

D = 6 mm

f ≅ 0.004

$\dot{Q}$ (W)	0.05	0.10	0.20	0.30	0.40	0.50	0.60	0.70
$\dot{m}$ (g/s)	0.27	0.53	1.02	1.45	1.82	2.14	2.43	2.68
ΔP (Pa)	0.017	0.065	0.24	0.48	0.76	1.05	1.35	1.66

ΔP_{max} = 70 Pa
$\dot{Q}_{max}$ = 77.22 W
$\dot{m}_{max}$ = 22.9 g/s
(f = 0.00231)

8.4.2 L = 30 m T = 1.4 K

D = 6 mm

f ≅ 0.004

$\dot{Q}$ (W)	0.05	0.1	0.2	0.3	0.5	0.7	1.0
$\dot{m}$ (g/s)	0.27	0.52	0.99	1.38	2.00	2.48	3.02
ΔP (Pa)	0.025	0.095	0.34	0.66	1.39	2.12	3.16

ΔP_{max} = 70 Pa
$\dot{Q}_{max}$ = 59.4 W
$\dot{m}_{max}$ = 18.1 g/s

8.4.3 L = 40 m T = 1.4 K

D = 6 mm

f ≅ 0.004

$\dot{Q}$ (W)	0.05	0.10	0.20	0.30	0.40	0.50	0.60	0.70
$\dot{m}$ (g/s)	0.27	0.54	1.05	1.53	1.95	2.35	2.70	3.00
ΔP (Pa)	0.008	0.03	0.12	0.25	0.42	0.61	0.80	1.00

ΔP_{max} = 70 Pa
$\dot{Q}_{max}$ = 112.9 W
$\dot{m}_{max}$ = 33.5 g/s
(f = 0.00231)

8.4.4 L = 20 m T = 1.5 K

D = 6 mm

f ≅ 0.004

$\dot{Q}$ (W)	0.05	0.1	0.2	0.3	0.4	0.5	0.6	0.7	0.8	0.9	1.0
$\dot{m}$ (g/s)	0.17	0.34	0.67	0.99	1.29	1.57	1.83	2.07	2.3	2.51	2.70
ΔP (Pa)	0.007	0.026	0.10	0.22	0.38	0.57	0.77	0.99	1.21	1.45	1.68

ΔP_{max} = 68 Pa
$\dot{Q}_{max}$ = 76.4 W
$\dot{m}_{max}$ = 22.6 g/s
(f = 0.0023)

8.4.5 L = 30 m T = 1.5 K

D = 6 mm

$\dot{Q}$ (W)	0.05	0.1	0.2	0.3	0.5	0.7	1.0
$\dot{m}$ (g/s)	0.17	0.34	0.66	0.97	1.51	1.97	2.54
ΔP (Pa)	0.01	0.04	0.15	0.33	0.80	1.35	2.22

ΔP_{max} = 68 Pa
$\dot{Q}_{max}$ = 61.3 W
$\dot{m}_{max}$ = 18.1 g/s

8.4.6 Conclusion

Let us refer to the case of L = 30 m and D = 6 mm as a representing one. For T = 1.4 K a heat power of about 0.45 W should be applied for reaching the 1.86 g/S flowrate. At T = 1.5 K it increases to about 0.65 W. Those required heat power supplies have to be compared to the (assumable) specified magnet dissipation: 0.01 W per coil. Comes out the conclusion that there is not enough driving heat power for supporting a significant external convection, and it becomes an internal convection case.

If we would consider an external supply of about 0.5 W to support that flowrate than we increase the total heat load and He II consumption by about one and a half order of magnitude which is not acceptable either.

8.5 Stability

The self-sustained FEP operation is a closed loop feedback system. As such it should be examined about the conditions of stability.

Hofmann describes[17] the first unsteady heat load experiment as undergoing strong oscillations. The pressure oscillated between zero and its maximum value by a time constant of about 150 especially in the low values of FEP driving heat powers. Hofmann reports that in order to ensure stable behavior an additional constant heat supply of about 0.5 W is required for complete suppression of the oscillations. That additional heat power seems to be incomparable to the 0.02 W magnet steady state dissipation.

A block diagram in Fig. 21 is suggested for system engineering analysis of the HLS. On its basis a stability condition might be derived for non-oscillating behavior.

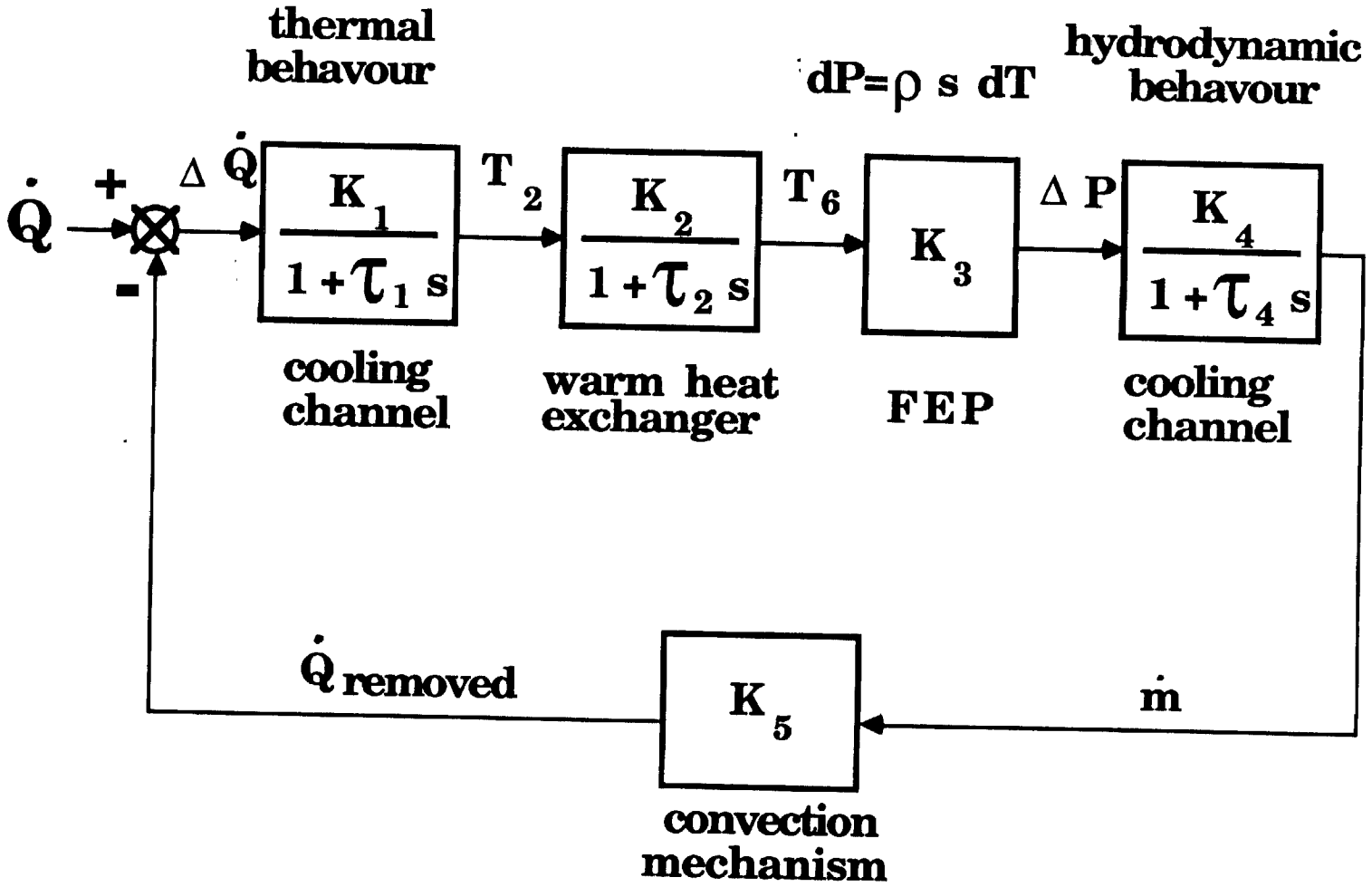

Fig. 21: Block diagram linearized representation of Hofmann's Cooling Loop for system stability analysis.

References

1. ASTROMAG facility definition, by J. F. Ormes, M. Israel, M. Wiedenbeck and R. Mewaldt, Aug. 1986.
2. Boyle, Robert F., Astromag Dewar Subsystem, Phase A, Study Report, November 3, 1989, NASA Goddard Space Flight Center, Code 713.1.
3. Astromag Coil Cooling Study (NASA).
4. Goodlang, J. S. and Irey, R. K., Non-boiling and film boiling heat transfer to a saturated bath of liquid helium, Adv. Cryo. Eng. 15, 299 (1970).
5. Green, M. A., Cryogenics, its influence on the selection of the ASTROMAG superconducting magnet coils.
6. Green, M. A., The two coil toroid magnet, an option for ASTROMAG.
7. Green, M. A. and Castles, S., Design concepts for the ASTROMAG cryogenic system, Adv. Cryo. Engn., 33, 631 (1988).
8. Brookhaven National Laboratory, Selected Cryogenic Data Notebook, Vol. 1, sections I - IX (Aug. 1980).
9. Egan, J. P., The Lorenz ratio of high purity aluminum in magnetic fields, Ph.D. thesis, University of Wisconsin-Madison, 1984.
10. Van Sciver, S. W., Nilles, M. J. and Pfotenhauer, J., Thermal and electrical conductance between metals at low temperatures, Space Cryogenics Workshop, Berlin, Germany, Aug. 7-9, 1984.
11. Van Sciver, S. W., Heat transport in forced flow He II: analytic solution, Adv. Cryo. Eng. 29, 315-322 (1984).

12. Van Sciver, S. W., "Helium Cryogenics", Plenum Press, New York (1986).

13. Maytal, B., Nissen, J. A. and Van Sciver, S. W., Interaction of He II transfer line and fountain effect pump, accepted for publication in Cryogenics.

14. Hofmann, A., Thermomechanically driven helium II flow. An option for fusion magnet swith internally cooled conductors, Proc. 11th Intern. Cryo. Engn. Conf., Berlin, West Germany, 22-25 April, 1986, pp. 306-11.

15. Hofmann, A., Khalil, A. and Krämer, H. P., Heat exchangers for He-II cooling loop with self-sustained fountain effect pumps, Cryogenics 27, 681-688 (1987).

16. Hofmann, A., Khalil, A. and Krämer, H. P., Operational characteristics of loops with helium II flow driven by fountain effect pumps, CEC/ICMC Conference, paper No. 585 (1987).

17. Hofmann, A. and Kasthurirengan, S., Fountain effect pump driven helium flow at steady and unsteady heat load, CEC/ICMC Conference, July 24-28, 1989, Los Angeles, USA, paper HA-01.

18. Eckert and Drake, Heat Transfer, McGraw Hill (1970).

19. Krämer, H. P., Heat transfer to forced flow in He II, Proc. 12th Intern. Cryo. Engn. Conf., Southampton, U.K., 12-15 July, 1988, pp. 299-304.

20. Weisend, J. G. and Van Sciver, S. W., Surface heat transfer measurements in forced flow He II in Superfluid Helium Heat Transfer, ASME publication H00587, pp. 1-8.

21. Walstrom, P. L., Weisend II, J. G., Maddocks, J. R. and Van Sciver, S. W., Turbulent flow pressure drop in various He II transfer system components, Cryogenics, 28, 101 (1988).